

EARLY ONLINE RELEASE

This is a PDF of a manuscript that has been peer-reviewed and accepted for publication. As the article has not yet been formatted, copy edited or proofread, the final published version may be different from the early online release.

This pre-publication manuscript may be downloaded, distributed and used under the provisions of the Creative Commons Attribution 4.0 International (CC BY 4.0) license. It may be cited using the DOI below.

The DOI for this manuscript is

DOI:10.2151/jmsj.2022-030

J-STAGE Advance published date: April 8th, 2022

The final manuscript after publication will replace the preliminary version at the above DOI once it is available.

1 **Heatstroke risk projection in Japan under current and**
2 **near future climates**

3
4
5
6 **Shingo NAKAMURA**

7 *Graduate School of Life and Environmental Sciences*
8 *University of Tsukuba, Tsukuba, Japan*

9
10 **Hiroyuki KUSAKA¹**

11 *Center for Computational Sciences*
12 *University of Tsukuba, Tsukuba, Japan*

13
14 **Ryogo SATO**

15 *Graduate School of Life and Environmental Sciences*
16 *University of Tsukuba, Tsukuba, Japan*
17 *Current affiliation: Sompō Risk Management Inc., Tokyo, Japan*

18
19
20 **and**

21
22 **Takuto SATO**

23
24 *Center for Computational Sciences*
25 *University of Tsukuba, Tsukuba, Japan*

26
27
28
29 **<Month> <day>, 2021**

30
31
32 -----
33 1) Corresponding author: Hiroyuki Kusaka, Center for Computational Sciences, University
34 of Tsukuba, 1-1-1, Tennodai, Tsukuba-shi, Ibaraki 305-8577 JAPAN.
35 Email: kusaka@ccs.tsukuba.ac.jp
36 Tel: +81-29-853-6481
37

Abstract

38
39
40
41
42
43
44
45
46
47
48
49
50
51
52
53
54
55
56
57
58
59
60

This study assesses heatstroke risk in the near future (2031-2050) under RCP8.5 scenario. The developed model is based on a generalized linear model with the number of ambulance transport due to heatstroke (hereafter the patients with heatstroke) as the explained variable and the daily maximum temperature or Wet-Bulb Globe Temperature (WBGT) as the explanatory variable. With the model based on the daily maximum temperature, we performed the projection of the patients with heatstroke in case of considering only climate change (Case 1), climate change and population dynamics (Case 2), and climate change, population dynamics, and long-term heat acclimatization (Case 3). In Case 2, the number of patients with heatstroke in the near future will be 2.3 times higher than that in the baseline period (1981-2000) on average nationwide. The number of future patients with heatstroke in Case 2 is about 10% larger than that in Case 1 on average nationwide despite of population decline. This is due to the increase in the number of elderly people from the baseline period to the near future. However, there were 21 prefectures where the number of patients in Case 2 is smaller compared to Case 1. Comparing the results from Cases 1 and 3 reveals that the number of patients with heatstroke could be reduced by about 60% nationwide by acquiring heat tolerance and changing lifestyles. Notably, given the lifestyle changes represented by the widespread use of air conditioners, the number of patients with heatstroke in the near future was lower than that of the baseline period in some areas. In other words, lifestyle changes can be an important adaptation to the risk of heatstroke emergency. All of the above results were also confirmed in the prediction model with WBGT as the explanatory variable. (291 words, Word limit is less than 300)

61 **Keywords:** Number of patients with heatstroke, Near future projection, Heat
62 acclimatization, Climate change adaptation, Generalized linear model (less than 5)

63
64
65
66
67
68
69
70
71
72
73
74
75
76
77
78
79
80
81
82
83
84
85
86
87
88

1. Introduction

In recent years, the incidence of heatstroke in Japan has increased due to climate change, and this is becoming a major social issue (e.g., Ando et al., 2004; Fujibe 2013). For example, from May to September 2018, which was abnormal hot summer across the country, the number of emergency patients with heatstroke was 95,137 nationwide, of which 32,496 were hospitalized and 160 died (Fire and Disaster Management Agency, 2019, https://www.fdma.go.jp/disaster/heatstroke/item/heatstroke003_houdou01.pdf). The number of deaths due to heatstroke in 2018 was 1,581. This number of deaths is far greater than the number of deaths caused by other weather-related disasters, such as floods and landslides (the number of deaths from the 2018 Japan floods, which were one of the most torrential in decades, was 225). Residents are concerned that heatstroke will become increasingly serious as climate change progresses. It is therefore important to assess all of the risks associated with heatstroke in a future climate.

Extensive studies on the increase in heat-related excess mortality or deaths associated with future climate change have been conducted mainly in Europe, the United States, Japan, and China (e.g., Hayhoe et al., 2004; Knowlton et al., 2007; Doyon et al., 2008; Gosling et al., 2009; Jackson et al. 2010; Li et al., 2013, Honda et al., 2014). Li et al. (2013) predicted that future heat-related excess deaths in New York, USA, under the Special Report on Emissions Scenarios (SRES) A2 scenario would increase by +22.2% (2020s), +49.4% (2050s), and +91.0% (2080s), compared to levels in the 1980s. Doyon et al. (2008) predicted a 10% increase in summer heat-related mortality in Montreal, Canada, in 2080 compared to that in 1981-1999 under the SRES A2 scenario. Similar studies have continued to be conducted after the release of the future climate projection datasets for the Representative Concentration Pathway (RCP) scenarios (Chen et al., 2017; Huber et al., 2020). In recent years, projections have also been conducted in developing countries, including those in

89 Southeast Asia. For example, Gasparrini et al. (2017) projected heat-related excess
90 mortality rates of more than 5% in Southeast Asia, central and southern Europe, and Latin
91 America in the 2090s under the RCP8.5 scenario. Guo et al. (2018) predicted that heat-
92 related deaths would increase by more than 700% in some countries of Southeast Asia and
93 South America during the period of 2031-2080 under the RCP8.5 scenario compared to the
94 1971-2020 period. Thus, future projections of heatstroke risk have been dominated by
95 studies that use heat-related excess mortality or deaths as indicators. In these studies, it is
96 necessary to consider not only climate change but also social change. Social changes
97 include demographic changes and long-term heat acclimatization over a span of several
98 decades due to lifestyle changes. Among the previous studies, those that consider
99 demographic changes are Gosling et al. (2009); Jackson et al. (2010); Honda et al. (2014);
100 Chen et al. (2017); Guo et al. (2018). Studies considering long-term heat acclimation are
101 Hayhoe et al. (2004); Knowlton et al. (2007); Gosling et al. (2009); Li et al. (2013); Guo et
102 al. (2018).

103 Therefore, the main purpose of this study is to develop a statistical model and predict
104 heatstroke risk (the number of ambulance transport due to heatstroke) in the near future
105 (2031-2050) under RCP2.6 and RCP8.5 scenarios all over Japan by prefecture. This
106 statistical model is based on the generalized linear model which uses maximum temperature
107 or WBGT as explanatory variable and daily number of ambulance transport due to
108 heatstroke as a predictor variable. When predicting the number of ambulance transport due
109 to heatstroke by statistical model, it is known that there is a problem of underestimation in
110 early summer and overestimation in late summer (Fuse et al., 2014; Sato et al., 2020; Ikeda
111 and Kusaka, 2021). This error is due to short-term heat acclimatization (Ono, 2013; Fujibe
112 et al., 2018b). Therefore, our model takes this effect into account. The near future heatstroke
113 risk is determined by three types of experiments. (i) Future projection considering only
114 climate change. (ii) Future projection considering climate change and population. (iii) Future

115 projection considering climate change, population and long-term acclimatization. The detail
116 information of experiments is described in section 3.
117

118 **2. Data**

119 *2.1 Number of heatstroke emergency patients*

120 In this study, we used a dataset on the number of ambulance transport due to heatstroke
121 for 2010 - 2018 published by the Fire and Disaster Management Agency of the Ministry of
122 Internal Affairs and Communications, Japan.

123 The definition of heat stroke is "a general term for any disorder that results from an
124 imbalance of water and salt (e.g. sodium) in the body due to a breakdown in the body's
125 ability to regulate the temperature in a high-temperature environment" and includes
126 sunstroke, heat cramps, heat exhaustion and heat stroke (Fire and Disaster Management
127 Agency 2021)". Based on the above definition, the medical doctor determines whether the
128 patient brought to the emergency room has a heatstroke. The data on the number of
129 emergency patients with heatstroke by that medical doctor's initial diagnosis is used in this
130 study. There are three types of age-related data in this dataset: the number of heatstroke
131 emergency patients per day by prefecture in all age groups, aged 65 years and older, and
132 under 64 years old (newborn babies, infants, juveniles, and adults combined). The number
133 of ambulance transport due to heatstroke is simply called "the number of patients with
134 heatstroke" and used as an indicator of heatstroke risk in this study.

135

136 *2.2. Current climate data*

137 The temperature data were taken from hourly observations made by the Automated
138 Meteorological Data Acquisition System (AMeDAS) operated by the Japan Meteorological
139 Agency. AMeDAS stations are located at a density of approximately 20 km. We used the
140 spatial average of all stations' values within a prefecture to improve the spatial
141 representativeness of the temperature value used for each prefecture. However, because
142 the climate of Tokyo differs markedly between the mainland and the islands, spatial averages
143 of Tokyo are calculated by excluding data from observation stations on the islands (these

144 islands have 0.2% of the total population of Tokyo). The daily maximum temperatures were
145 determined from the hourly temperature values obtained from these averages.

146 WBGT was calculated using the formula of Yaglou and Minard (1957). The black globe
147 temperatures there are not measured by JMA were estimated by the method of Okada and
148 Kusaka, 2013. The daily maximum WBGT was calculated from the hourly values of WBGT.
149 Detailed methods for estimating the WBGT are described in the Supplement 1.

150

151 *2.3 Climate scenario data*

152 As the climate scenario data, we used the 1-km mesh statistical downscaling (DS) dataset
153 provided by Institute for Agro-Environmental Sciences, National Agriculture and Food
154 Research Organization (NARO) (Nishimori et al., 2019). This DS dataset were created from
155 four GCMs outputs, MIROC5, MRI-CGCM3, GFDL-CM3, and HadGEM2-ES. These GCMs
156 were carefully selected by SI-CAT, project for climate change adaptation in Japan. For the
157 period of climate scenarios used in this study, the baseline period is set to 1981-2000 and
158 the near future is set to 2031-2050.

159 Unfortunately, the NARO dataset stores only data for daily (mean, maximum, minimum)
160 and monthly mean values, not store hourly values. Due to this limitation, it is impossible to
161 calculate the daily maximum WBGT with only this dataset. In addition, it should be noted
162 that the reliability of each meteorological variable differs. To be honest, it is reported that
163 the reliability of air temperature and solar radiation is relatively high, while that of humidity
164 and wind speed is relatively low (Nishimori et al., 2019).

165 A similar idea as the pseudo-global warming approach (Kimura and Kitoh 2007, Sato et al
166 2007) was applied to estimate the future WBGT to overcome these problems in this study.
167 First, a time series of daily maximum temperature from June 1 to September 30 is
168 generated using the baseline period data from NARO's dataset. Second, this time series is
169 averaged over 15 days and then averaged over 10 years. Third, similar time series data is

170 generated using the future climate scenario data of NARO's dataset. From the difference
171 between these two-time series, we obtain the climate change component data (ΔT). This
172 ΔT is daily data of the amount of temperature increase from the present to the future, which
173 contains a gentle seasonal change. The pseudo future dry-bulb temperature is estimated
174 from the actual temperature of the present climate T plus future temperature increase ΔT .
175 The pseudo future WBGT is estimated using pseudo future dry-bulb temperature ($T+\Delta T$),
176 wet-bulb temperature (T_w) and globe temperature (T_g). Here, the future T_w should be
177 calculated from the future relative humidity and the pseudo future temperature ($T+\Delta T$).
178 However, in this study, pseudo future T_w is calculated from the current relative humidity
179 and the pseudo future temperature, considering the result of the previous study that the
180 relative humidity does not change significantly in Japan in the near future (Byrne and
181 O'Gorman 2016). Similarly, the pseudo future T_g is calculated from the current solar
182 radiation, wind speed and the pseudo future temperature.

183

184 *2.4 Population data*

185 As the current (baseline) population data by prefecture, we used the data from the 1990
186 Population Census. As the future population data by prefecture, we used the "Future
187 Population Estimates by Region for Japan" provided by the National Institute of Population
188 and Social Security Research (National Institute of Population and Social Security Research
189 2018). This dataset is a statistical future projection of the population by prefecture and
190 municipality. This data is suitable for the purpose of this study because it is estimated by
191 age group (0-14 years, 15-64 years, 65 years and older, and 75 years and older).

192 The population data here is the nighttime population for both base and near-future values.
193 If the population of a prefecture is expressed using nighttime population, there will be an
194 error in the risk of heatstroke if a person suffers from heatstroke during the daytime in a
195 prefecture other than his or her home. However, this error is expected to have only a little

196 effect on the predictions of this study for the following two reasons. The first reason is that
197 the difference between the daytime and nighttime populations is small except in a few
198 prefectures. According to the 2005 census, the difference between the daytime and
199 nighttime population is about 20% even in Tokyo, where the daytime population is much
200 larger than the nighttime population, and about 12% even in Saitama, where the daytime
201 population is much smaller than the nighttime population. In other prefectures, the difference
202 between the daytime and nighttime populations was less than 10%. Another reason is that
203 most of the people suffering from heatstroke are young children and the elderly. Since the
204 difference between the daytime and nighttime populations occurs mainly in the age group
205 that commutes to work or school, these are different age groups from the young children
206 and elderly.

207

208 **3. Method**

209 **3.1 Model overview**

210 In this study, the six models shown in Table 1 were created and compared for accuracy.
211 The characteristics of the proposed models for the number of patients with heatstroke
212 prediction are as follows:

- 213 (i) The model is based on generalized linear models (GLM, Nelder and Wedderburn, 1972).
- 214 (ii) The predictor variable is the number of heatstroke emergency patients.
- 215 (iii) The default explanatory variable is the daily maximum temperature. (but, we can also
216 use WBGT instead).
- 217 (iv) Differences in regional, seasonal (short-term heat acclimatization), and age of
218 heatstroke risk were considered when identifying the model parameters.

219

220 Regarding (i), GLM equation is expressed as follows.

221

$$222 \log(y) = \alpha + \beta x \quad (1)$$

223

224

225 Here, x is the explanatory variable, y is the objective variable, and α and β are partial
226 regression coefficients (parameters). Each parameter was identified by the maximum
227 likelihood method, which assumes a Poisson distribution. First, as a default model, we
228 created a model with the estimated parameters using data from Tokyo and adapted the
229 model to the entire country.

230 Regarding (ii), the results of this model will provide useful information for examining the
231 requirements of the emergency medical system in consideration of the increase in the
232 number of patients with heatstroke due to future climate change.

233 Regarding (iii), it is expected that the use of the daily maximum temperature leads to a
234 high practicality in making future predictions. This is because the humidity, wind speed and
235 solar radiation used in the WBGT estimation have tendency with lower availability and

236 robustness of future climate scenario data, compared with temperature. On the other hand,
237 WBGT is possibly more suitable for explanatory variables under current climate than
238 temperature. These pros/cons are trade-off relationship for future projection; thus, we
239 compare the accuracies between the two models; the one uses the temperature as the
240 explanatory variable and the other uses the WBGT. And then, we individually predict future
241 heatstroke risk using the two models. The comparison of such models might be important
242 attempt to understand the uncertainty among prediction models.

243 Regarding (iv), it is expected that the proposed model will improve the accuracy of the future
244 projection of the number of emergency transport due to heatstroke by considering the factors
245 not limited to the meteorological field. We will describe these factors in the subsection 3.2 –
246 3.4 in detail.

247

248 *3.2. Consideration of regional dependency in the model*

249 The degree of heat tolerance of people is known to vary among regions (Keatinge et al.,
250 2000; Curriero, 2002; Gosling et al., 2007; Fujibe et al., 2018a). For example, when exposed
251 to the same temperature, people in the cooler regions of northern Japan have a higher risk
252 of heatstroke than people in warmer regions (Fujibe et al., 2018a). To account for these
253 regional differences in heat tolerance, we performed parameter estimation for each
254 prefecture individually.

255

256 *3.3 Consideration of short-term heat acclimatization in the model*

257 The predictions calculated from equation (1) are problematic in that they underestimate
258 the predictions in the early summer and overestimate the predictions in the late summer.
259 This is because the effect of short-term acclimatization is not included when using a single
260 equation as described before. Like Ikeda and Kusaka (2021), using an actual number of
261 patients with heatstroke one day before and the cumulative days from the start of summer

262 season as explanatory variables is an example of ways to consider the short-term
263 acclimatization effect. However, the actual number of patients with heatstroke is not able to
264 use under the future climate projection. Cumulative days might be useful idea in the future
265 projection because it indicates the number of hot days experienced in one summer. However,
266 it cannot be applied to the model in this study because the timing of mid-summer may
267 change in the long term, and in that case, simple cumulative days may not be able to
268 represent this change.

269 In this study, we propose the method to divide the predicted period from June to
270 September into three sub-periods: early summer, mid-summer, and late summer, based on
271 the time series of daily maximum temperature (Fig. 1). The equations are respectively
272 constructed for early summer and late summer using data in these sub-periods (equation 2
273 and 3) to consider the effect of short-term acclimatization. These equations are respectively
274 used in early summer and late summer instead of equation (1).

$$275$$
$$276 \log(y_{p1}) = \alpha_{p1} + \beta_{p1}x \quad (2)$$

$$277 \log(y_{p3}) = \alpha_{p3} + \beta_{p3}x \quad (3)$$
$$278$$

279 As mentioned above, if equation (1) is used for the entire summer, it will underestimate
280 the number of emergency cases in early-summer and overestimate the number of
281 emergency cases in late-summer. In this study, in order to mitigate these errors, we divided
282 the period into three parts, focusing on the temperature increase from early-summer to mid-
283 summer and the temperature decrease from mid-summer to late-summer. The period
284 division was carried out using the values of [posterior five-day mean minus previous five-
285 day mean] (hereafter referred to as the “five-day mean difference”). This five-day mean
286 difference represents the trend of temperature change in about 10 days. When temperature

287 rises over a span of about 10days, five-day mean difference shows positive value. The
288 method of period division is as follows. The example of this method is shown in Figure 1.

289

- 290 ● Start date of the early-summer period: June 1
- 291 ● End date of the early-summer period: 7 days after the last day when the value of the
292 five-day mean difference exceeded the threshold. This end date is picked from the
293 period from June 1 to August 9. The thresholds are 50th to 95th percentile of the five-
294 day mean difference and set by prefectures. For example, at Fukuoka in 2018, the end
295 date of the early-summer period is set to August 9 (the end of the period shown in orange
296 in Fig.1). If the date selected is on or after August 10, the end date of the early-summer
297 period is uniformly set to August 9. This is because the tendency to underestimate the
298 prediction values generally finishes by early August in any year.
- 299 ● Start date of the late-summer period: The date when the value of five-day mean
300 difference falls below the threshold for the first time during the period August 10 –
301 September 30. The thresholds are fifth to 50th percentile of the five-day mean difference
302 and set by prefectures. For example, at Fukuoka in 2018, the start date of the late-
303 summer period is set to August 14th (the start of the period shown in blue in Fig. 1).
- 304 ● End date of the late-summer period: September 30
- 305 ● Mid-summer period: From the day after the end of the early summer period to the day
306 before the start of the late summer period (the period shown in green in Fig. 1). In mid-
307 summer period, the error in the predictions based on the non-division model is enough
308 small and there is no need to revise them.

309

310 *3.4. Consideration of differences in patient's age in the model*

311 It is well known that the risk of heatstroke is higher in the elderly than in the young (Nakai
312 et al., 1999; Smoyer et al., 2000; McGeehin and Mirabelli, 2001; Basu and Samet, 2002;

313 Flynn et al., 2005; Hajat et al., 2007; Anderson and Bell, 2009). Therefore, to account for
314 these differences in heatstroke risk by age, we separately predicted the number of patients
315 with heatstroke 65 and older and under 64 years of age (Figure 2).

316

317 *3.5. Factors not considered in the model*

318 The following factors related to the heatstroke risk are not used in the prediction model.

319 (i)sex (Semenza et al., 1996; Whitman et al., 1997; Havenith, 2005; Vaidyanathan et al.,
320 2020), (ii) use of air conditioners or air conditioner penetration rate (Semenza et al., 1996;
321 Basu and Samet, 2002; Anderson and Bell, 2009), and (iii) socioeconomic status (Anderson
322 and Bell, 2009; Hondula et al., 2015; Fujibe et al., 2020), (iv) whether they are living in a
323 nursing home or not (Kovats and Hajat 2008), (v) clinical or pathophysiological factors, (vi)
324 urban heat islands (Kovats and Hajat 2008), and (vii) air pollution levels (Piver et al. 1999).

325 (i) Sex could not be considered in this study because the dataset on the number of
326 heatstroke emergency patients used in this study did not distinguish between men and
327 women.

328 (ii) The penetration rate of air conditioners is around 90% in most prefectures, except in a
329 few areas. The presence or absence of air conditioner use may have something to do with
330 the presence or absence of heatstroke occurrence, but it is difficult to obtain such data at
331 the national level. For this reason, this factor is not used in the prediction model.

332 As for (iii) and (iv), in Japan there is almost no gap between the rich and the poor, and
333 social security and medical insurance are almost well provided for all citizens. This leads
334 that air conditioners are considered to be sufficiently widespread for nursing care facilities.
335 Regarding (v), predicting what will happen to the number of people with diseases related to
336 heat stroke risk in the future (whether it will increase or decrease) is highly uncertain and
337 unrealistic. Regarding (vi), Japan's cities are already mature, and it is unlikely that further

338 urbanization will enhance the heat island effect (Adachi et al. 2012, Kusaka et al. 2016).
339 Regarding (iiv), the effect of air pollutants on heatstroke is smaller than the effect of
340 temperature (e.g., Shumway et al., 1988, Smoyer et al., 2000, Rainham and Smoyer-Tomic
341 2003). The impact of air pollutants on heatstroke in Toronto 1980-1996 was small (Rainham
342 and Smoyer-Tomic 2003). During that period, the NO₂ concentration in Toronto was 0.0238
343 ppm, while the NO₂ concentration in Tokyo in 2018 was 0.015 ppm, which is lower than that
344 in Toronto. In addition, air pollutants in Tokyo have been decreasing in recent years and are
345 expected to continue to do so in the future (Morikawa et al., 2021). Therefore, air pollutants
346 are not considered in this study.

347 In addition, this study did not consider the geospatial population density pattern within a
348 prefecture. However, if it is considered, the risk of heatstroke can be assessed in more
349 spatial detail. This will be useful information for the optimal allocation of medical facilities.

350

351 *3.6. Changing explanatory variables in the model*

352 The thermal indices, WBGT (Yaglou and Minard, 1957), and Universal Thermal Climate
353 Index (UTCI; Fiala et al., 2012), are widely used to measure heatstroke risk in the world. In
354 Japan, WBGT are the most widely used and also recognized as an effective guideline for
355 work and exercise environments. Moreover, WBGT has been standardized internationally
356 by the International Organization for Standardization. The UTCI is often used worldwide, but
357 its application to Japanese people is considered questionable as it is based on the
358 physiological responses of Caucasian human models. In this study, we used the daily
359 maximum WBGT as explanatory variable as well as daily maximum temperature, and
360 investigated the effect of different explanatory variables on the prediction accuracy.

361

362 *3.7. Verification of model accuracy*

363 Cross-validation was performed with any one year of data from 2010-2018 as test data
364 and the remaining eight years as training data. The predictive accuracy of the models was
365 assessed by mean absolute error (MAE) and root mean squared error (RMSE), and models
366 with small values of each of these parameters was considered to have higher predictive
367 accuracy.

368

369 3.8. Design of Baseline and near-future projection

370 First, we will estimate the number of patients with heatstroke in Baseline period (1981-
371 2000) using statistical models developed in chapter 3 by prefecture. Second, we will perform
372 the future projection of heatstroke risk in Japan by prefecture. The heatstroke risk in this
373 study means the number of patients with heatstroke, as described in Section 1. We use
374 Model 6 in table 1 for future projection of the number of patients with heatstroke. We perform
375 two sensitivity experiments (Cases 2 and 3) in addition to control experiment (Case 1) to
376 discuss the uncertainty of future projection results. The future projection experiments are
377 summarized in Table 2.

378

- 379 ● Case 1: Future projection considering neither near future demographics nor long-term
380 acclimatization into account.
- 381 ● Case 2: Future prediction considering only the near future demography.
- 382 ● Case 3: Future prediction considering both near future demography and long-term
383 acclimatization.

384

385 Case 1 is an experiment to evaluate the increase in the risk of heatstroke due solely to
386 the increase in temperature caused by climate change. In this experiment, the number of
387 patients with heatstroke in the entire region is used as the risk indicator, but it is assumed
388 that the demographics will not change between now and the future. In other words, the

389 increase in risk in this experiment is the same as the increase in the risk of heat stroke for
390 each individual resident.

391 Case 2 is an experiment to evaluate the variation in the risk of heatstroke by considering
392 the temperature increase due to climate change and demographic change from the baseline
393 period to the near future. In this experiment, we can obtain the projected number of patients
394 with heatstroke for the entire region at each time point in the baseline period and near future.
395 Thus, this future projection is able to assess the risks related to the burden on the emergency
396 medical system associated with an increase in the number of patients with heatstroke. The
397 burden on the emergency medical system refers specifically to the shortage of emergency
398 transport systems and inpatient beds, as indicated in Chapter 1. Therefore, it is expected
399 that the results of this future projection will be very useful information for the government to
400 formulate adaptation measures to climate change.

401 It is known that heat acclimatization can occur over a long period of time, apart from
402 short-term acclimatization throughout the single summer. Petkova et al. (2014) noted that
403 the excess mortality observed between 1973 and 2006 was much lower than that observed
404 between 1900 and 1948, indicating that people have become acclimatized to the heat during
405 this period. They concluded that this acclimatization is due to the improvement of the living
406 environment and the widespread use of air conditioners. Therefore, in this study, the
407 following experiments (a) and (b) are conducted to evaluate long-term heat acclimatization
408 from the baseline to the near future. In both Case 3a and Case 3b were considered
409 population dynamics.

410

411 (a) An experiment in which individuals are assumed to have heat tolerance equivalent to late
412 summer throughout one summer season (Case 3a).

413 (b) An experiment using a climate analogue to account for lifestyle changes in a cold region
414 with particularly low air conditioning penetration (Case 3b).

415

416 In the prediction experiment of Case 3a, we particularly examine the effect of long-term
417 acclimatization due to the acquisition of heat tolerance. Equation (3) for late summer,
418 described in 3.3, is used to predict the number of patients with heatstroke in near future over
419 the entire summer period, including early and mid-summer. This is based on the assumption
420 that the government and individuals will have heat tolerance equivalent to that of late
421 summer throughout the entire summer period by taking all kinds of heat countermeasures.

422 In the prediction experiment of Case 3b, we examined the effects of long-term
423 acclimatization due to the acquisition of heat tolerance and lifestyle changes. In this
424 experiment, targeting the areas are Hokkaido, Aomori, Iwate, Miyagi, Akita, Yamagata,
425 Fukushima, Nagano, and Yamanashi. These areas have low percentages of households
426 with air conditioning during the baseline period. We first looked for the three prefectures of
427 that the current daily maximum temperature is the close to the near future daily maximum
428 temperature of a target prefecture. And then, using the prediction models of the selected
429 three prefectures, the near-future projections were made for the target prefecture. This
430 procedure was finally conducted for nine target prefectures with low air conditioner
431 penetration rate today. This method is a kind of the climate analog approach (e.g., Ishizaki
432 et al. 2012). This near-future prediction is based on the assumption that the inhabitants of
433 the regions with low air-conditioner penetration rates in the baseline period will acquire the
434 same heat tolerance or change their lifestyles as those of other regions with similar climates
435 in the near future.

436 The targeting nine prefectures (Hokkaido, Aomori, Iwate, Miyagi, Akita, Yamagata,
437 Fukushima, Nagano, and Yamanashi) had particularly low air conditioner penetration rates
438 in 1999 (specifically, 9.3% in Hokkaido, 30.2% in Aomori, 35.6% in Iwate, 59.1% in Miyagi,
439 56.7% in Akita, 67.8% in Yamagata, 58.4% in Fukushima, 44.8% in Nagano, and 72.0% in
440 Yamanashi). The air conditioner penetration rates in the other prefectures are all above 80%

441 (based on the 1999 National Survey of Actual Consumption, [https://www.e-](https://www.e-stat.go.jp/dbview?sid=0000111013)
442 [stat.go.jp/dbview?sid=0000111013](https://www.e-stat.go.jp/dbview?sid=0000111013)).

443 The future projections are carried out using daily maximum WBGT instead of daily
444 maximum temperature as an explanatory variable. The method of calculating the daily
445 maximum WBGT in baseline and near-future is described in Section 2.3 and Supplement 1.

446

447 **4. Accuracy of the proposed statistical models under the current climate**

448 *4.1 Improvement in model accuracy by considering regional and short-term heat*
449 *acclimatization and age*

450 First, we developed a model to predict the number of heatstroke emergency patients using
451 the daily maximum temperature data for Tokyo and conducted prediction experiments and
452 accuracy verification (cross-validation) for each prefecture (Model 1). The prediction errors
453 of the Model 1 were 5.5 (MAE) and 10.6 (RMSE), on average, across the country.

454 Second, we performed prediction with Model 3 and compared the results between Models
455 1 and 3. As a result, it was confirmed that the MAE could be reduced by about -19% (-46%
456 to -3% in each prefecture) and the RMSE by about -25% (-48% to -0% in each prefecture)
457 on average, across the country by taking into account regional characteristics (Figure 3).

458 As the third experiment, we performed prediction with Model 5 and compared the results
459 between Models 3 and 5. We found that, from the results, considering the short-term heat
460 acclimatization (i.e., effect of Model 5) reduced the MAE by about 12% (-22% to -3% in each
461 prefecture) and the RMSE by about 12% (-20% to -4% in each prefecture) on average,
462 across the country.

463 Last, we compared errors between the odd-numbered model group (Models 1, 3, 5) with
464 the even-numbered model group (Models 2, 4, 6), indicating that the prediction accuracy on
465 average, across the country remained almost unchanged when differences in risk by age
466 were considered.

467 We explicitly show the effect of improving the accuracy due to considering the period
468 division (i.e., Model 5 effect) using data for 2018 Fukuoka Prefecture (one of the major
469 prefectures in Japan) as an example from the cross-validation results. In 2018, a severe
470 heat wave was experienced across Japan. Thus, predicting the number of patients with
471 heatstroke in 2018 using climate data from 2010-2017 is a good example for a prediction

472 experiment for a warmer future using standard summer data. The results showed that the
473 early summer period is characterized by having a relatively high number of patients with
474 heatstroke and the late summer period is characterized as having relatively fewer patients
475 (Figure 4). Note that it was also confirmed in many prefectures other than Fukuoka. Figure
476 4 shows the time series of daytime predictions obtained from the model with and without
477 period division and benchmark model (i.e., Models 1, 3, vs 5). It can be seen that the model
478 without period division (Model 3) significantly underestimates the peak in the number of
479 patients from early July to early August. It also tends to overestimate the peak in mid to late
480 August. On the other hand, these tendencies of underestimation and overestimation are
481 greatly improved in the model with period division (Model 5) (32% reduction in MAE and
482 29% reduction in RMSE).

483 484 *4.2 Effect of different explanatory variables on prediction accuracy*

485 The explanatory variables with the highest prediction accuracy for each region were
486 investigated for the predictions obtained using Model 6. From the perspective of MAE
487 (Figure 5), the daily maximum WBGT would be selected as the best explanatory variable in
488 27 of the 46 regions. From the perspective of RMSE (Figure 6), the daily maximum WBGT
489 would be selected as the best explanatory variable in 31 of the 46 regions. These results
490 suggest that WBGT is better explanatory variable than daily maximum temperature for
491 predicting the number of patients with heatstroke. This is consistent with studies that have
492 shown that humidity is an important explanatory variable for heatstroke risk (Zhang et al,
493 2014; Sherwood, 2018). However, in the majority of prefectures, the difference in the error
494 between the temperature models and WBGT models was less than 10%, with a maximum
495 of 20% (MAE) and 25% (RMSE).

496

5. Future projection of the number of patients with heatstroke

5.1 Baseline

The estimated total number of patients with heatstroke per summer (averaged for 20 years x 4 GCMs) for the Baseline period is shown in Figure 7. This figure shows that the average total number of patients with heatstroke in all prefectures is 3.8/10,000 per summer, with a spread from a maximum of 6.3/10,000 (Kagoshima) to a minimum of 1.6/10,000 (Hokkaido) by prefecture. This spread reflects the regionality of both the temperature spread and tolerance to the heat.

5.2 Result of near future projection only effect of climate change: Case 1

Figure 8(a) shows a map of future changes in the risk of heatstroke (for Case 1). This figure indicates that the average total number of patients with heatstroke in all prefectures is 8.9/10,000 per summer, with a large spread from the maximum value of 18.6/10,000 (Kagoshima) to the minimum value of 5.2/10,000 (Tokyo) by prefecture.

Figure 9 shows the rate of increase in the number of patients with heatstroke from the baseline period (1981-2000) to the near future (for Case 1) on the averaged nationwide. This figure indicates that the number of patients with heatstroke in the near future will be 1.2-2.9 times (2.1 times in the ensemble average of 4 GCMs) in the case of RCP2.6 scenario and 1.4-3.3 times (2.2 times in the ensemble average of 4 GCMs) in the case of RCP8.5 compared to the baseline period. This range of values is due to the uncertainty of the GCMs; since there is no significant difference in the prediction results between the RCP2.6 and RCP8.5 scenarios because of near future projection, we will only discuss the prediction results for RCP8.5 from now on. The regions with the highest increase in the heat stroke risk from the baseline period to the near future are found to be Hokkaido, northern Tohoku, southern Kanto, Tokai, and Kyushu (Fig. 10a) (see Fig.A1 in Supplement 2 for the names of Japanese prefectures and regional categories). The prefecture with the highest rate of

523 increase was Hokkaido, with 313.6%. One of the reasons for this may be that Hokkaido has
524 experienced a larger increase in temperature due to climate change (about 2.2°C increase)
525 than other regions (see Fig.A2(a) in Supplement 3).

526 527 *5.3 Result of future projection with population dynamics: Case 2*

528 The risk map of patients with heatstroke in the near future (2031-2050) obtained from
529 the future prediction experiment of Case 2 is shown in Figure 8(b). This figure indicates that
530 the total number of patients with heatstroke nationwide is 9.6/10,000 per summer, with a
531 large spread from a maximum of 20.4/10,000 (Kagoshima) to a minimum of 5.7/10,000
532 (Tokyo) by prefecture.

533 A map of the increase rate in the number of patients with heatstroke from baseline to the
534 near future (under RCP8.5 scenario) for each prefecture of Case 2 is shown in Fig. 10 (b).
535 The increase rate on the average nationwide in the number of patients with heatstroke from
536 baseline period to the near future on the average nationwide obtained from Case 2 is 234.4%
537 in the ensemble mean of four GCMs. This increase rate on the average nationwide is about
538 10% larger than that in Case 1. The reason must come from the differences between Cases
539 1 and 2, that is (i) the increase in total population from the baseline to the near future, (ii)
540 the increase in the elderly population, or (iii) both. Let us now consider which of these three
541 factors was dominant. The population of Japan in the baseline (1990) is about 120 million,
542 while the population in the near future (2040) will be about 110 million. Therefore, if the
543 experiment only considers the increase or decrease in population, the number of patients
544 with heatstroke in Case 2 should be smaller than in Case 1. This means that the reason for
545 the increase the number of patients with heatstroke is the increase in the elderly population.
546 In fact, the proportion of elderly people in the total population has almost tripled from 12.0%
547 to 35.3% from baseline to near future. In all prefectures, the increase rate was higher than
548 100%. We can see that the increase rate is high in the prefectures with large population that

549 include the Tokyo metropolitan area and other major urban areas. Among these prefectures,
550 the difference in the prediction between Case 1 and Case 2 is the largest in Tokyo. In Tokyo,
551 the rate of future increase is 360.0% in Case 2, but 239.3% in Case 1. The population of
552 Tokyo as a whole increase by 16.6% from baseline to the near future, and the aging rate
553 also increases by 18.6% from baseline to the near future. In other words, in Tokyo, the risk
554 of heatstroke in Case 2 was particularly high compared to Case 1 due to two effects; total
555 population increase and increase in the aging rate from the baseline period to the near future,
556 in addition to climate change.

557 The demographic changes from the baseline to the near future can be classified into the
558 following four patterns for each prefecture.

559

560 (1) The population of the prefecture increases, and the proportion of elderly people in the
561 total population also increases. (Tokyo type)

562 (2) The population of the prefecture increases, but the proportion of elderly people in the
563 total population decreases.

564 (3) The population of the prefecture decreases, but the proportion of elderly people in the
565 total population increases.

566 (4) The population of the prefecture decreases, and the proportion of elderly people in the
567 total population decreases.

568

569 In type (1), the number of patients with heatstroke is definitely higher in Case 2 than Case
570 1 where only the temperature increase due to climate change is considered. However, in the
571 case of type (3), the results of future projections will depend on whether the decline in
572 population or the increase in the aging rate is dominant. There were no prefectures that
573 corresponded to type (2) and (4) (i.e., prefectures where the population aging rate decreases
574 from baseline to the near future).

575 As a result of comparing Case 2 and Case 1, we found that there were 26 prefectures
576 out of 46 prefectures where the number of patients with heatstroke was higher in Case 2.
577 Of the 26 prefectures, 6 prefectures including Tokyo were classified as type 1 (Tokyo-type).
578 In these prefectures, the number of patients with heatstroke will increase due to the following
579 three factors: (1) climate change, (2) population growth, and (3) increase in the aging
580 population. The remaining 20 prefectures were classified as type 3. In these prefectures, the
581 number of patients with heatstroke will increase due to climate change and an increase in
582 the aging population. Among these 20 prefectures, Fukuoka will have the highest increase
583 rate. In Fukuoka Prefecture, the increase in the number of patients with heatstroke from
584 baseline to the near future in Case 2 was estimated 289.8% (compared to 236.5% in Case
585 1).

586 In contrast to the prefectures belonging to the type 1 or type3 (e.g., Tokyo and Fukuoka),
587 21 of the 46 prefectures had a lower number of patients with heatstroke in Case 2 than in
588 Case 1. The largest difference in the prediction between Cases 1 and 2 was observed in
589 Akita Prefecture, where the increase in Case 2 was only 174.8%, but 235.9% in Case 1. In
590 other words, the risk in Case 2 is 61.1% lower than in Case 1. Focus on demographic
591 changes in Akita, the total population will decrease by 45.2% from the baseline period to the
592 near future, while the population aging rate will increase by 31.9%. This situation has both
593 a restraining effect on the number of patients with heatstroke (population decline) and an
594 increasing effect on the number of patients with heatstroke (aging of the population). In the
595 case of Akita, this restraining effect was dominant, which may have resulted in a lower
596 number of patients with heatstroke in Case 2 than in Case 1. Thus, demographic changes
597 have the effect of increasing or decreasing the number of patients with heatstroke, which is
598 an important consideration for future projections (Table 3).

599

600 *5.4 Result of near future projection with consideration of long-term acclimatization: Case 3*

601 The map of the near-future projection for Case 3a is shown in Figure 8(c). This figure
602 shows that the average total number of patients with heatstroke for all prefectures is 7.3 per
603 summer, with a wide range from a maximum of 14.7 per 10,000 people (Kagoshima) to a
604 minimum of 3.9 per 10,000 people (Tokyo) by prefecture.

605 Figure 10(c) shows a map of the average increase rate in the number of patients with
606 heatstroke in each prefecture in Case 3a. The average increase rate on average nationwide
607 is 164.5 %. This is about 60% smaller than Case 1, where only the effect of temperature
608 increase due to climate change is considered. In Hokkaido, where the increase in the
609 number of patients with heatstroke from baseline to the near future was the highest in Case
610 1, the value in Case 3a was reduced by about 100% compared to Case 1.

611 The map of the near-future projection for Case 3b is shown in Figure 8(d). This figure
612 shows that the average total number of patients with heatstroke in the nine prefectures is
613 5.3 people per summer, with a spread from a maximum of 10.1 people/10,000 people
614 (Yamanashi) to a minimum of 1.4 people/10,000 people (Hokkaido) by prefecture. Figure
615 10(d) shows a map of the increase rate in the number of patients with heatstroke from the
616 baseline period to the near future for Case 3b. The average value for the nine prefectures is
617 119.7%. In four of the nine prefectures, the number of emergency heatstroke cases
618 decreased compared to the current climate (Hokkaido: 66.0%, Miyagi: 85.3%, Yamagata:
619 77.0%, and Fukushima: 92.6%, assuming the value of baseline to be 100%).

620

621 *5.5 Near future projections with explanatory variables changed to daily maximum WBGT*
622 *(with population dynamics)*

623 Fig. 11 shows the map of number of patients with heatstroke when the same
624 assumptions as in Case 1, Case 2, Case 3a, and Case 3b are made and the explanatory
625 variable is changed to the daily maximum WBGT to predict the number of patients with
626 heatstroke in near future. Taking Case 2 (experiment considering demographics) as an

627 example, the total number of patients with heatstroke is 10.4/10,000 per summer nationwide,
628 with a large spread from the maximum value of 18.2/10,000 (Saga) to the minimum value of
629 5.1/10,000 (Hokkaido). The difference in the prediction between the model with daily
630 maximum WBGT and the model with daily maximum temperature is only about 9%. This
631 result suggests that there is no significant difference in the prediction results of the two
632 models when we focus on the number of patients with heatstroke nationwide. However,
633 looking at each prefecture, there are some prefectures where the results of near-future
634 prediction between the daily maximum temperature model and the daily maximum WBGT
635 model is largely different (Tables A1(a), A1(b) in Supplement 4).

636

637 **6. Conclusions**

638 The main aim of this study was to estimate the number of ambulance transport due to heat
639 stroke under the current and near future climates with a newly developed statistical model.
640 The model proposed in this study has the following three characteristics:

641

642 1) The dependent variable (predictor) was set as the number of heatstroke emergency
643 patients. Directly predicting the number of emergency patients allows us to assess, not only
644 the risk of heatstroke incidence among people, but also the burden on the emergency
645 medical system.

646 2) The daily maximum temperature, which is readily available from future climate prediction
647 datasets, was selected as an explanatory variable.

648 3) The seasonality of heatstroke risk (short-term heat acclimatization) was considered by
649 dividing the summer period into three sub-periods: early summer, mid-summer, and late
650 summer, with parameter identification appropriate for each period.

651

652 The proposed model considers not only temperature but also three main factors —region,
653 short-term heat acclimatization, and age— that are considered to affect the prediction
654 accuracy. The results of cross-validation showed that the prediction error was reduced by
655 about 22% and 12% respectively due to considering regional characteristics and short-term
656 heat acclimatization. On the other hand, it was found that the age did not much contribute
657 to the model accuracy.

658 In order to confirm the practicality and validity of the proposed model, we compared its
659 accuracy with models in which the explanatory variables were changed from the maximum
660 temperature to WBGT. The model with WBGT was the most accurate in the majority of
661 prefectures. However, the difference in the prediction error between the model with
662 temperature and the model with WBGT was less than 10% in the majority of prefectures.

663 We therefore conclude that models using maximum temperatures instead of the WBGT as
664 the explanatory variable can be used in practical situations by considering regional
665 differences and short-term heat acclimatization.

666 With the statistical model developed, three near-future projections of the heatstroke risk
667 were made: one considering only temperature increase due to climate change (Case 1), one
668 considering temperature increase due to climate change and demographic change (Case
669 2), and one considering temperature increase due to climate change, demographic change,
670 lifestyle change, and long-term heat acclimatization (Case 3a, b). In Case 1, the risk of
671 heatstroke from the perspective of residents increases by about 2.2 times from baseline to
672 the near future on the average nationwide (the ensemble means of 4 GCMs under the
673 RCP8.5 scenario). The increase in risk was particularly pronounced in Hokkaido, where the
674 risk of heatstroke increase was greater than three times. The risk of heatstroke from the
675 perspective of the government in Case 2 increased by a factor of 2.3 from baseline to the
676 near future on the average nationwide. This result suggests that the burden of heatstroke
677 emergency cases on the emergency medical system in the near future cannot be ignored.
678 The heatstroke risk in the near future in Case 2 is greater than that in Case 1 on the average
679 nationwide. However, there were some prefectures such as in Akita that the effect of
680 population decline on risk reduction is more dominant than the climate change on risk
681 increase. Whether demographic change increases or decreases risk is not uniquely
682 determined. From the prediction of Case 3a, it is found that the risk of emergency heatstroke
683 can be reduced by about 30% on average nationwide by acquiring heat tolerance and
684 changing lifestyles.

685 Lifestyle changes mean various changes for the adaptation to the worse thermal
686 environment, as represented by the widespread use of air conditioners. See Section 3.8 for
687 details. Case 3b shows that the risk of emergency heatstroke in the near future is lower

688 than that in the baseline in some regions, such as Hokkaido. In other words, the results
689 suggest that there is much room for risk control in cold regions by promoting the acquisition
690 of heat tolerance and lifestyle changes.

691 Finally, in order to confirm the uncertainty of the explanatory variables, a comparison
692 experiment was conducted using the daily maximum WBGT as an explanatory variable. As
693 a result, the difference between the prediction result of the number of patients with
694 heatstroke by the daily maximum temperature model and that by the daily maximum
695 temperature WBGT model was about 9% on average nationwide.

696

697

698 **Data Availability Statement**

- 699 ● The number of ambulance transport datasets analyzed in this study are available at
700 [<https://www.fdma.go.jp/disaster/heatstroke/post3.html>].
- 701 ● The current climate data (AMeDAS) analyzed in this study are available at
702 [<https://www.data.jma.go.jp/gmd/risk/obsdl/>].
- 703 ● The statistical downscaling datasets (Nishimori et al., 2019) analyzed in this study are
704 available at [doi:10.20783/DIAS.568].
- 705 ● The population datasets analyzed in this study are available at [Baseline (1990);
706 <https://www.e-stat.go.jp/dbview?sid=0000031399>] and [Near future (2040);
707 <https://www.ipss.go.jp/pp-shicyoson/j/shicyoson18/t-page.asp>].
- 708 ● The datasets generated and analyzed in this study (TableA1) are available at
709 [<https://doi.org/10.2151/jmsj.2022-030>].

710

711

712 **Supplement**

713 *Supplement 1: How to calculate the maximum daily WBGT*

714 In this study, the following equation was used to calculate WBGT (Yaglou and Minard, 1957).

715 Day and night were discriminated based on the value of horizontal-plane insolation; a
716 positive horizontal-plane insolation value was judged to be daytime and zero was judged to
717 be nighttime.

718

719 $WBGT = 0.7T_w + 0.2T_g + 0.1T_d$ (daytime)

720 $WBGT = 0.7T_w + 0.3T_d$ (nighttime)

721

722 The dry-bulb and wet-bulb temperatures were based on the aforementioned values. The
723 black-bulb temperature (T_g) was estimated using the equation by Okada and Kusaka (2013).

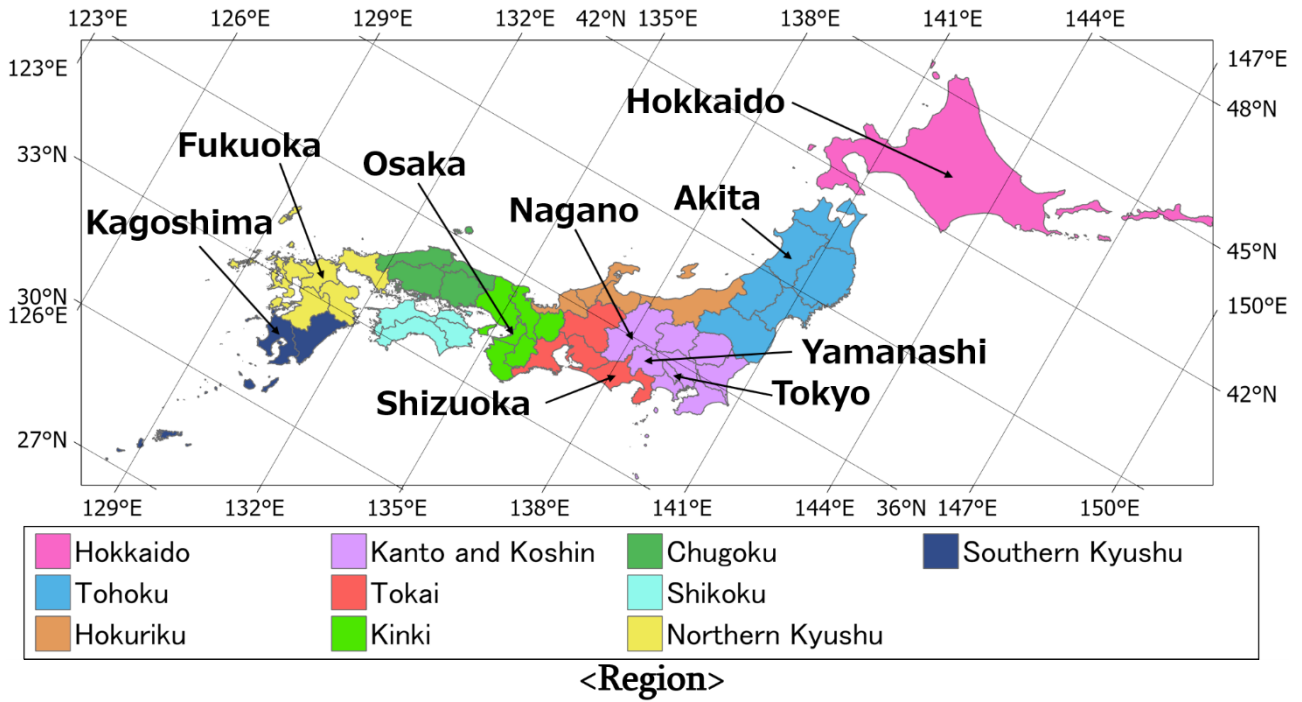
724 When using this equation, the values of wind speed and solar radiation are also required.

725 The wind speed was the spatial average of AMeDAS observations, as well as the
726 temperature. Solar radiation was measured by the meteorological observatory. However,
727 some meteorological observatories do not observe insolation. In such cases, the values
728 were estimated from the time series of sunshine duration using the equation by Kondo
729 (1994) and Kondo and Xu (1997). The daily maximum WBGT was obtained from the hourly
730 values of WBGT obtained using this method.

731

732

734



735

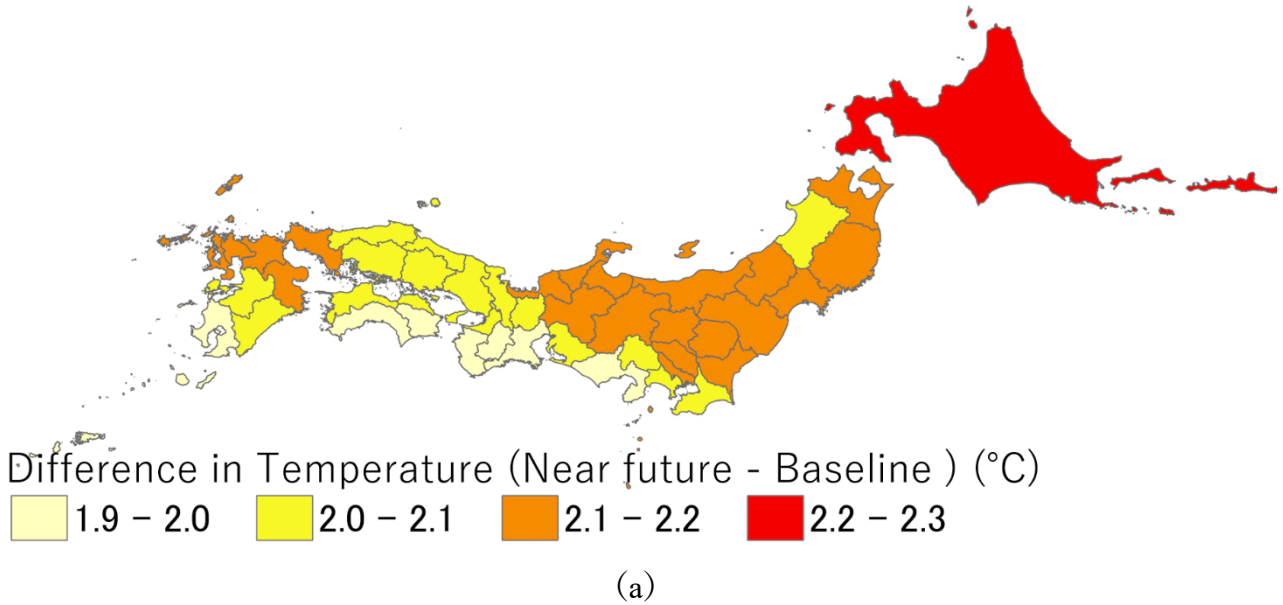
736

737 Fig. A1: Regional classifications and names of major prefectures in Japan. Based on the
738 forecast categories used in the JMA's regional seasonal forecasts. Note that this
739 classification is slightly different from the standard classification by the government.

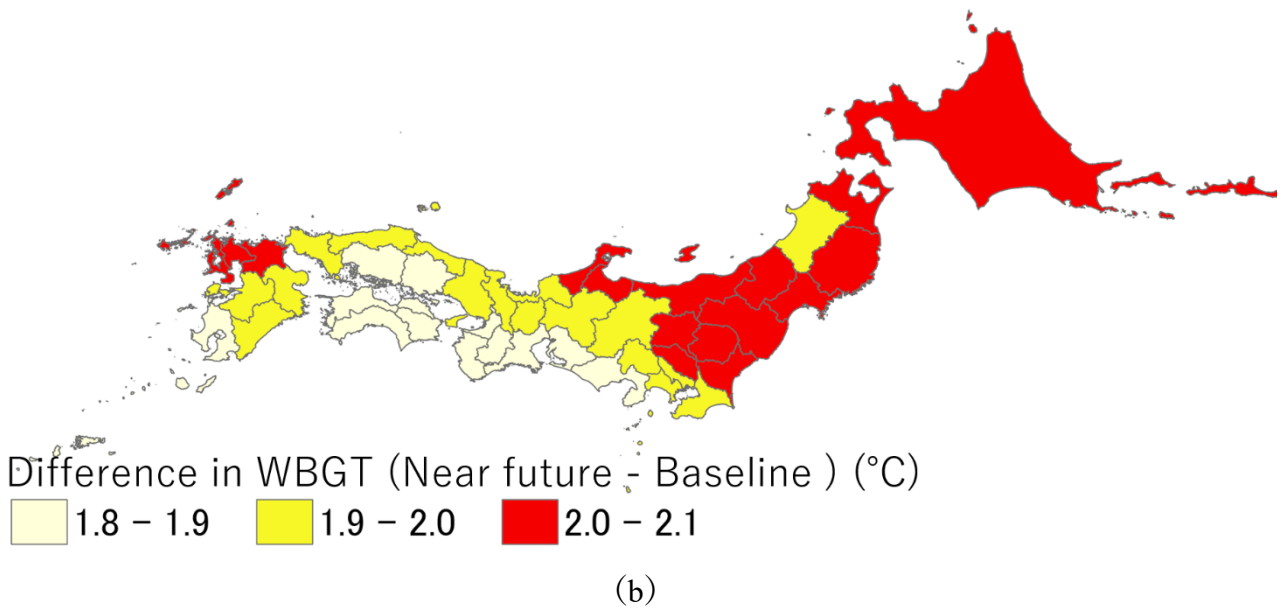
740

741 *Supplement 3: Increase in daily maximum temperature and daily maximum WBGT from*
742 *the baseline period to the near future period*

743



744
745



746
747

748 Fig. A2: Increase in (a) daily minimum temperature and (b) daily maximum WBGT (°C) from
749 the baseline period to the near future period for each prefecture. Daily maximum
750 temperature and daily maximum WBGT were ensemble averages from four GCMs,
751 GFDL-CM3, HadGEM2-ES, MIROC5, and MRI-CGCM3 (RCP8.5).

752

753 *Supplement 4:* The number of people transported to emergency rooms for heat stroke in
 754 each experiment (Beseline, Case1, Case2, Case3a and Case3b) and the days with high
 755 risk of heat stroke.

756

757 Table A1: The number of heatstroke emergency patients in summer and days with high
 758 risk of heat stroke in each prefecture predicted in this study. (a) explanatory variable is
 759 daily maximum temperature, (b) daily maximum temperature is daily maximum WBGT.
 760 The days with high risk of heat stroke are (a) extremely hot days (daily maximum
 761 temperature $\geq 35^{\circ}\text{C}$) and (b) dangerous days (daily maximum WBGT $\geq 31^{\circ}\text{C}$).

762

763

764

(a)

Pref.	Number of extremely hot days	Number of extremely hot days	Number of patients with heatstroke	Number of patients with heatstroke	Number of patients with heatstroke	Number of patients with heatstroke	Number of patients with heatstroke
	Beseline	Near future	Baseline	Near future (Case 1)	Near future (Case 2)	Near future (Case 3a)	Near future (Case 3b)
Hokkaido	0.0	0.6	914.9	3018.1	3385.5	914.9	603.5
Aomori	0.1	1.7	381.3	888.1	1108.3	381.3	493.3
Iwate	0.3	2.6	433.9	907.4	1099.2	433.9	595.9
Miyagi	0.3	2.1	590.6	1483.2	1603.9	590.6	504.1
Akita	0.5	5.1	432.8	756.5	1026.5	432.8	607.7
Yamagata	0.6	5.8	373.1	715.9	873.5	373.1	287.3
Fukushima	0.2	3.9	832.4	1654.7	1924.8	832.4	770.9
Ibaraki	1.2	10.5	922.6	2117.5	2368.9	922.6	—
Tochigi	0.1	3.4	566.9	1389.8	1523.9	566.9	—
Gunma	1.0	9.6	833.6	1901.2	2095.3	833.6	—
Saitama	11.0	33.9	1865.9	5624.3	5515.4	1865.9	—

Chiba	0.7	10.1	1620.3	5109.1	5225.9	1620.3	—
Tokyo	2.8	17.0	2161.1	7778.3	7058.8	2161.1	—
Kanagawa	0.5	9.8	1587.4	5777.3	5652.2	1587.4	—
Niigata	0.6	8.4	954.2	1892.4	2222.5	954.2	—
Toyama	1.2	14.2	272.2	567.0	646.5	272.2	—
Ishikawa	0.6	9.7	399.6	951.5	1025.2	399.6	—
Fukui	1.7	18.0	257.2	539.4	605.5	257.2	—
Yamanashi	1.8	14.5	281.1	597.1	689.8	281.1	653.9
Nagano	0.0	1.9	594.3	1328.1	1482.3	594.3	690.4
Gifu	0.9	12.6	729.0	1559.9	1773.2	729.0	—
Shizuoka	0.5	7.1	2039.9	5479.4	6064.3	2039.9	—
Aichi	2.8	23.3	2326.4	7074.3	6831.0	2326.4	—
Mie	1.9	16.8	731.1	1748.5	1950.8	731.1	—
Shiga	0.8	12.0	361.2	1081.2	1070.5	361.2	—
Kyoto	4.8	29.4	1096.2	2686.3	2836.2	1096.2	—
Osaka	3.2	27.1	2899.6	7405.1	7854.7	2899.6	—
Hyogo	1.2	16.3	2194.9	5853.7	6099.3	2194.9	—
Nara	2.1	15.4	571.6	1126.4	1317.7	571.6	—
Wakayama	0.2	4.7	600.4	1052.8	1294.9	600.4	—
Tottori	1.2	11.1	290.7	547.6	620.4	290.7	—
Shimane	0.6	7.4	339.1	607.1	716.3	339.1	—
Okayama	1.9	15.9	1024.9	2244.6	2403.7	1024.9	—

Hiroshima	0.7	8.1	1079.9	2508.1	2630.9	1079.9	—
Yamaguchi	0.8	10.1	594.8	1161.8	1423.0	594.8	—
Tokushima	0.4	7.4	330.6	623.8	748.6	330.6	—
Kagawa	3.6	27.5	504.0	1123.1	1247.9	504.0	—
Ehime	0.4	8.6	706.1	1398.7	1641.3	706.1	—
Kochi	0.1	3.2	426.1	802.7	1013.2	426.1	—
Fukuoka	2.1	21.4	1555.5	4508.4	4535.8	1555.5	—
Saga	4.0	26.6	456.4	941.9	1062.3	456.4	—
Nagasaki	0.0	2.7	705.7	1485.0	1763.3	705.7	—
Kumamoto	1.1	17.9	955.9	2115.4	2333.3	955.9	—
Oita	0.6	9.5	511.1	1068.7	1210.6	511.1	—
Miyazaki	0.8	10.9	620.5	1316.0	1533.3	620.5	—
Kagoshima	0.1	3.2	1126.5	2622.2	3066.6	1126.5	—

765

766

767

768

769

(b)

Pref.	Number of dangerous days	Number of dangerous days	Number of patients with heatstroke	Number of patients with heatstroke	Number of patients with heatstroke	Number of patients with heatstroke	Number of patients with heatstroke
	Baseline	Near future	Baseline	Near future (Case 1)	Near future (Case 2)	Near future (Case 3a)	Near future (Case 3b)
Hokkaido	0.0	0.1	753.0	2047.3	2169.6	1463.9	532.9
Aomori	0.2	2.2	300.5	763.2	679.0	499.6	760.4
Iwate	0.0	2.1	350.3	888.3	818.5	567.7	964.5
Miyagi	0.2	5.5	579.9	1507.2	1746.5	1208.7	1317.7
Akita	0.3	5.3	353.7	891.8	669.6	603.8	983.2
Yamagata	0.0	4.1	362.1	910.9	802.5	583.6	773.4
Fukushima	0.0	1.4	692.2	1692.2	1619.2	1156.0	1035.1
Ibaraki	3.1	18.7	1052.6	2708.6	2885.0	2324.7	—
Tochigi	0.0	4.2	521.7	1340.6	1482.1	1214.6	—
Gunma	0.2	5.3	792.6	1999.4	2126.4	1625.8	—
Saitama	4.4	23.9	2149.4	5376.9	7803.5	5795.4	—
Chiba	1.5	18.5	1770.2	4624.7	6051.3	5148.1	—
Tokyo	0.0	6.2	2382.9	7860.8	12166.3	7247.1	—
Kanagawa	0.5	13.0	1557.1	4639.6	6581.0	4792.1	—
Niigata	1.0	12.7	852.0	2112.8	1970.5	1623.1	—
Toyama	0.6	15.0	243.8	611.5	622.3	474.0	—
Ishikawa	0.4	10.2	418.1	1108.9	1216.8	1044.5	—
Fukui	0.0	10.2	211.0	571.3	580.1	452.5	—
Yamanashi	0.0	5.7	305.4	750.3	767.7	557.1	912.5

Nagano	0.0	0.7	430.6	992.1	1,030	800.1	894.0
Gifu	0.1	7.3	866.8	2103.3	2135.1	1587.0	—
Shizuoka	0.1	6.3	1031.0	2538.5	2771.2	2356.6	—
Aichi	0.4	13.7	2342.4	6075.4	8717.1	6534.6	—
Mie	3.2	21.2	785.8	2009.3	2094.4	1526.7	—
Shiga	2.8	19.6	349.0	814.9	1106.3	828.2	—
Kyoto	0.1	12.6	1006.6	2341.9	2783.6	2077.8	—
Osaka	0.3	10.7	2329.8	6048.6	7166.3	5834.3	—
Hyogo	1.2	16.5	1787.2	4162.9	5088.0	4088.8	—
Nara	0.4	14.9	587.9	1341.2	1331.5	1076.8	—
Wakayama	0.2	8.6	511.4	1119.4	950.2	676.4	—
Tottori	0.0	5.8	263.9	697.2	661.8	541.5	—
Shimane	0.1	11.2	312.5	755.8	668.9	527.1	—
Okayama	0.4	9.1	925.7	2168.4	2400.3	1919.7	—
Hiroshima	0.6	14.2	1353.9	3061.8	3456.4	2112.2	—
Yamaguchi	4.1	25.4	514.4	1321.1	1096.8	822.5	—
Tokushima	2.4	20.3	347.5	784.5	719.3	578.7	—
Kagawa	2.2	25.7	492.2	1200.9	1241.2	875.8	—
Ehime	0.4	14.1	678.6	1604.7	1480.7	1192.3	—
Kochi	0.9	12.3	317.4	762.0	634.0	468.5	—
Fukuoka	4.3	28.3	1352.9	3613.8	4513.7	3612.8	—
Saga	4.5	30.6	533.8	1364.0	1264.9	909.5	—

Nagasaki	0.3	13.8	599.1	1537.8	1366.3	1179.6	—
Kumamoto	0.6	20.4	844.3	2263.9	2293.8	1882.5	—
Oita	2.0	23.6	531.6	1297.2	1317.9	957.3	—
Miyazaki	3.2	26.6	479.7	1161.5	1104.8	904.3	—
Kagoshima	0.6	19.8	842.6	2089.3	1911.8	1530.9	—

770

771

772

773

774

775

Acknowledgments

776

777

778

779

780

781

782

783

784

785

786

787

788

789

790

791

792

793

794

795

796

797

798

799

800

This work was supported by the Social Implementation Program on Climate Change Adaptation Technology (SI-CAT) Grant Number JPMXD0715667165 from the Ministry of Education, Culture, Sports, Science and Technology (MEXT), Japan. This research was performed by the Environment Research and Technology Development Fund JPMEERF20192005 of the Environmental Restoration and Conservation Agency of Japan.

References

- Adachi, A., F. Kimura, H. Kusaka, T. Inoue, and H. Ueda, 2012: Comparison of the Impact of Global Climate Changes and Urbanization on Summertime Future Climate in the Tokyo Metropolitan Area. *J. Appl. Meteor. Climatol.*, **51**, 1441-1454.
- Anderson, B. G., and M. L. Bell, 2009: Weather-related mortality How heat, cold, and heat waves affect mortality in the United States. *Epidemiology*, **20**, 205-213.
- Ando, M., S. Yamamoto, S. Asanuma, 2004: Global Warming and Heatstroke. *Japanese Journal of Biometeorology*, **41(1)**, 45-49 (in Japanese with English abstract).
- Basu, R., and Samet, J. M. 2002: An exposure assessment study of ambient heat exposure in an elderly population in Baltimore, Maryland. *Environmental health perspectives*, **110(12)**, 1219-1224.
- Byrne, M. P. and P. A. O’Gorman, 2016: Understanding Decreases in Land Relative Humidity with Global Warming: Conceptual Model and GCM Simulations. *Journal of Climate*, **29**, 9045-9061.
- Chen, K., R. M. Horton, D. A. Bader, C. Lesk, L. Jiang, B. Jones, L. Zhou, X. Chen, J. Bi, P. L. Kinney, 2017: Impact of climate change on heat-related mortality in Jiangsu Province, China. *Environmental Pollution*, **227**, 317-325.

801 Curriero, F. C., K. S. Heiner, J. M. Samet, S. L. Zeger, L. Strug, and J. A. Patz, 2002:
802 Temperature and mortality in 11 cities of the eastern United States. *American journal of*
803 *epidemiology*, **155(1)**, 80-87.

804 Doyon, B., D. Bélanger, and P. Gosselin, 2008: The potential impact of climate change on
805 annual and seasonal mortality for three cities in Québec, Canada. *International journal*
806 *of health geographics*, **7(1)**, 1-12.

807 Fiala, D., G. Havenith, P. Bröde, B. Kampmann, and G. Jendritzky, 2012: UTCI-Fiala multi-
808 node model of human heat transfer and temperature regulation. *International journal of*
809 *biometeorology*, **56(3)**, 429-441.

810 Fire and Disaster Management Agency, Ministry of Internal Affairs and Communications,
811 2021: *Commencement of "Survey on the number of people transported to emergency*
812 *rooms due to heatstroke during the summer"*, 2pp (in Japanese). [Available at
813 https://www.fdma.go.jp/disaster/heatstroke/items/heatstroke_chousa_kyu124.pdf.]
814 (Accessed on February 17, 2022).

815 Flynn, A., C. McGreevy, and E. C. Mulkerrin, 2005: Why do older patients die in a
816 heatwave? *Q. J. Med.*, **98**, 227-229.

817 Fujibe, F., 2013: Long-term Variations in Heat Mortality and Summer Temperature in
818 Japan. *Tenki*, **60(5)**, 371-381 (in Japanese with English abstract).

819 Fujibe, F., J. Matsumoto, and H. Suzuki, 2018a: Spatial and temporal features of heat
820 stroke mortality in Japan and their relation to temperature variations, 1999–2014.
821 *Geographical review of Japan series B*, **91(1)**, 17-27.

822 Fujibe, F., J. Matsumoto, and H. Suzuki, 2018b: Regional features of the relationship
823 between daily heat-stroke mortality and temperature in different climate zones in Japan.
824 *SOLA*, **14**, 144-147.

825 Fujibe, F., J. Matsumoto, and H. Suzuki, 2020: Spatial Variability of Municipality-wise Heat
826 and Cold Mortality in Japan with Respect to Temperature and Economic States.
827 *Geographical review of Japan series B*, **92(2)**, 72-83.

828 Fuse, A., S. Saka, R. Fuse, T. Araki, S. Kin, M. Miyauchi, and H. Yokota, 2014: Weather
829 data can predict the number of heat stroke patient. *Journal of Japanese Association for*
830 *Acute Medicine*, **25**, 757–765 (in Japanese with English abstract).

831 Gasparrini, A., et al., 2017: Projections of temperature-related excess mortality under
832 climate change scenarios. *The Lancet Planetary Health*, **1(9)**, e360-e367.

833 Gosling, S. N., G. R. McGregor, and A. Páldy, 2007: Climate change and heat-related
834 mortality in six cities Part 1: model construction and validation. *Int. J. Biometeorol.*, **51**,
835 525-540.

836 Gosling, S. N., G. R. McGregor, and J. A. Lowe, 2009: Climate change and heat-related
837 mortality in six cities Part 2: climate model evaluation and projected impacts from
838 changes in the mean and variability of temperature with climate change. *International*
839 *journal of biometeorology*, **53(1)**, 31-51.

840 Guo Y, A. et al., 2018: Quantifying excess deaths related to heatwaves under climate
841 change scenarios: A multicountry time series modelling study. *PLoS Med.*, **15(7)**:
842 e1002629.

843 Hajat, S., R. S. Kovats, and K. Lachowycz, 2007: Heat-related and cold-related deaths in
844 England and Wales: who is at risk?. *Occupational and environmental medicine*, **64(2)**,
845 93-100.

846 Hajat, S., M. O'Connor, and T. Kosatsky, 2010: Health effects of hot weather: from
847 awareness of risk factors to effective health protection. *The Lancet*, **375(9717)**, 856-
848 863.

849 Havenith, G., 2005: Temperature regulation, heat balance and climatic stress. In Extreme
850 weather events and public health responses (pp. 69-80). Springer, Berlin, Heidelberg.

851 Hayhoe, K., D. Cayan, C. B. Field, P. C. Frumhoff, E. P. Maurer, N. L. Miller, S. C. Moser,
852 S. H. Schneider, K. N. Cahill, E. E. Cleland, L. Dale, R. Drapek, R. M. Hanemann, L. S.
853 Kalkstein, J. Lenihan, C. K. Lunch, R. P. Neilson, S. C. Sheridan, and J. H. Verville,
854 2004: Emissions pathways, climate change, and impacts on California. *Proceedings of*
855 *the national academy of sciences*, **101(34)**, 12422-12427.

856 Honda, Y., M. Kondo, G. McGregor, H. Kim, Y. L. Guo, Y. Hijioka, M. Yoshikawa, K. Oka, S.
857 Takano, S. Hales, and R. S. Kovats, 2014: Heat-related mortality risk model for climate
858 change impact projection. *Environmental health and preventive medicine*, **19(1)**, 56-63.

859 Hondula D. M., R. E. Davis, M. V. Saha, C. R. Wegner, and L. M. Veazey, 2015:
860 Geographic dimensions of heat-related mortality in seven U.S. cities. *Environ. Res.*, **138**,
861 439-452.

862 Huber, V., L. Krummenauer, C. Peña-Ortiz, S. Lange, A. Gasparrini, A.M. Vicedo-Cabrera,
863 R. Garcia-Herrera, and K. Frieler, 2020: Temperature-related excess mortality in
864 German cities at 2 °C and higher degrees of global warming, *Environ. Res.*, **186**,
865 109447.

866 Ikeda, T., and H. Kusaka, 2021: Development of models for predicting the number of
867 patients with heatstroke on the next day considering heat acclimatization. *J. Meteor.*
868 *Soc. Japan.*, **99(6)**, 1395-1412.

869 Ishizaki, N., H. Shiogama, K. Takahashi, S. Emori, K. Dairaku, H. Kusaka, T. Nakaegawa,
870 and I. Takayabu 2012: An attempt to estimate of probabilistic regional climate analogue
871 in a warmer Japan. *J. Meteor. Soc. Japan*, **90B**, 65-74. doi:10.2151/jmsj.2012-B05

872 Jackson, J. E., M. G. Yost, C. Karr, C. Fitzpatrick, B. K. Lamb, S. H. Chung, J. Chen, J.
873 Avise, R. A. Rosenblatt, R. A. Fenske, 2010: Public health impacts of climate change in
874 Washington State: projected mortality risks due to heat events and air pollution. *Climatic*
875 *Change*, **102**, 159-186.

876 Kasai, M., T. Okaze, A. Mochida, and K. Hanaoka, 2017: Heatstroke risk predictions for
877 current and near-future summers in Sendai, Japan, based on mesoscale WRF
878 simulations, *Sustainability*, **9**, 1467.

879 Keatinge, W. R., G. C. Donaldson, E. Cordioli, M. Martinelli, A. E. Kunst, J. P.
880 Mackenbach, S. Nayha, I. Vuori, 2000: Heat related mortality in warm and cold regions
881 of Europe: observational study. *Bmj*, **321(7262)**, 670-673.

882 Kimura, F. and A. Kitoh, 2007: Downscaling by pseudo global warming method. In The
883 Final Report of the ICCAP. *Research Institute for Humanity and Nature (RIHN)*, Kyoto,
884 Japan.

885 Knowlton, K., B. Lynn, R. A. Goldberg, C. Rosenzweig, C. Hogrefe, J. K. Rosenthal, and P.
886 L. Kinney, 2007: Projecting heat-related mortality impacts under a changing climate in
887 the New York City region. *American journal of public health*, **97(11)**, 2028-2034.

888 Kovats, R. S. and S. Hajat, 2008: Heat stress and public health: a critical review, *Annu.*
889 *Rev. Public Health*, **29**, 41-55.

890 Kusaka, H., A. Suzuki-Parker, T. Aoyagi, S. A. Adachi, Y. Yamagata, 2016: Assessment of
891 RCM and urban scenarios uncertainties in the climate projections for August in the
892 2050s in Tokyo, *Climatic Change*, **137(3)**, 427-438.

893 Li, T., R. M. Horton, P. L. Kinney, 2013: Projections of seasonal patterns in temperature-
894 related deaths for Manhattan, New York. *Nature Climate change*, **3**, 717-721.

895 McGeehin, M. A., and M. Mirabelli, 2001: The potential impacts of climate variability and
896 change on temperature-related morbidity and mortality in the United States.
897 *Environmental health perspectives*, **109(suppl 2)**, 185-189.

898 Morikawa T., H. Yamada, K. Tanaka, S. Okayama Y. Shibata, Y. Nakata, H. Watanabe,
899 and T. Kidokoro, 2021: Air Quality Estimation in 2050 – JSAE 2050 Challenge and

900 Air Quality Estimation in 2050 – . *Transactions of the Society of Automotive Engineers*
901 *of Japan, Inc.* **52(6)**, 1261-1266, (in Japanese).

902 Nakai, S., T. Itoh, and T. Morimoto, 1999: Deaths from heat-stroke in Japan: 1968–1994.
903 *International journal of biometeorology*, **43(3)**, 124-127.

904 National Institute of Population and Social Security Research 2018: Regional Population
905 Projections for Japan: 2015-2045, 256pp [Available at [https://www.ipss.go.jp/pp-](https://www.ipss.go.jp/pp-shicyoson/j/shicyoson18/6houkoku/houkoku.asp)
906 [shicyoson/j/shicyoson18/6houkoku/houkoku.asp](https://www.ipss.go.jp/pp-shicyoson/j/shicyoson18/6houkoku/houkoku.asp)] (in Japanese)

907 Nelder, J. A., and R. W. Wedderburn, 1972: Generalized linear models. *Journal of the*
908 *Royal Statistical Society: Series A (General)*, **135(3)**, 370-384.

909 Nishimori, M., Y. Ishigooka, T. Kuwagata, T. Takimoto, N. Endo, 2019: SI-CAT 1km-grid
910 square regional climate projection scenario dataset for agricultural use (NARO2017).
911 *Journal of the Japan society for simulation technology*, **38**, 150-154, (in Japanese).

912 Okada, M., and H. Kusaka, 2013: Proposal of a new equation to estimate globe
913 temperature in an urban park environment. *Journal of Agricultural Meteorology*, **69(1)**,
914 23-32.

915 Ono, M. 2013: Heat stroke and the thermal environment. *JMAJ-Japan Medical Association*
916 *Journal*, **56(3)**, 199-205.

917 Piver, W. T., M. Ando, F. Ye, C. J. Portier, 1999: Temperature and air pollution as risk
918 factors for heat stroke in Tokyo, July and August 1980-1995. *Environmental Health*
919 *Perspectives*, **107**, 911-916.

920 Petkova. E. P., A. Gasparri, and P. L. Kinney, 2014: Heat and mortality in New York City
921 since the beginning of the 20th century, *Epidemiology*, **25**, 554-560.

922 Rainham, D. G. C., and K. E. Smoyer-Tomic, 2003: The role of air pollution in the
923 relationship between a heat stress index and human mortality in Toronto. *Environmental*
924 *research.*, **93**, 9–19.

925 Sato T., F. Kimura, and A. Kitoh, 2007: Projection of global warming onto regional
926 precipitation over Mongolia using a regional climate model. *Journal of Hydrology*, **333**,
927 144–154.

928 Sato, T., H. Kusaka, and H. Hino, 2020: Quantitative assessment of the contribution of
929 meteorological variables to the prediction of the number of patients with heatstroke for
930 Tokyo. *SOLA*, **16**, 104–108

931 Semenza J. C., C. H. Rubin, K. H. Falter, J. D. Selanikio, D. Flanders, H. L. Howe, and J.
932 L. Wilhelm, 1996: Heat-related deaths during the July 1995 heat wave in Chicago. *The*
933 *New England J. Medicine*, **335**, 84–90.

934 Sharwood, S. C., (2018). How important is humidity is heat stress? *Journal of Geophysical*
935 *Research: Atmospheres*, **123**, 11808-11810.

936 Shumway, R. H., A. S. Azari, and Y. Pawitan, 1988: Modeling mortality fluctuations in Los
937 Angeles as functions of pollution and weather effects. *Environmental research.*, **45**,
938 224–241.

939 Smoyer, K. E., D. G. Rainham, and J. N. Hewko, 2000: Heat-stress-related mortality in five
940 cities in Southern Ontario: 1980–1996. *International Journal of Biometeorology*, **44(4)**,
941 190-197.

942 Smoyer, K. E., L. S. Kalkstein, J. S. Greene, and H. Ye, 2000: The impacts of weather and
943 pollution on human mortality in Birmingham, Alabama and Philadelphia, Pennsylvania.
944 *International Journal of Climatology.*, **20**, 881-897.

945 Whitman, S., G. Good, E. R. Donoghue, N. Benbow, W. Shou, and S. Mou, 1997: Mortality
946 in Chicago attributed to the July 1995 heat wave. *American Journal of public health*,
947 **87(9)**, 1515-1518.

948 Vaidyanathan, A., J. Malilay, P. Schramm, and S. Saha, 2020: Heat-Related Deaths—
949 United States, 2004–2018. *Morbidity and Mortality Weekly Report*, **69(24)**, 729.

950 Yaglou, C. P., and D. Minard, 1957: Control of heat casualties at military training centers,
951 *American Medical Association Archives of Industrial Health*.

952 Zhang, K., Y. Li, J. D. Schwartz, and M. S. O'Neill, 2014: What weather variables are
953 important in predicting heat-related mortality? A new application of statistical learning
954 methods. *Environ. Res.*, **132**, 350–359.

955

956

957

List of Figures

958

959 Fig. 1 An example of period division used in this study.

960

961 Fig. 2 Scatterplot showing the relationship between the daily maximum temperature and
962 the number of patients in Fukuoka Prefecture in 2018. Red, green, and blue plots
963 indicate early summer, mid-summer, and late summer periods, respectively. The lines
964 are prediction equations fitted from the data indicated by the plots. The scatterplot (a)
965 shows the number of patients who are under 65 years of age. The scatterplot (b)
966 shows the number of patients who are 65 years of age or older. The scatterplot (c)
967 shows the number of patients who are all ages.

968

969 Fig. 3 (a) MAE and (b) RMSE of the number of patients in 2018 predicted using each
970 model. Box whiskers represent the range in values obtained for 46 regions. To remove
971 the effect of population size, MAE and RMSE were plotted as normalized values per
972 10,000 people.

973

974 Fig. 4 Time series of the daily maximum temperature and actual and predicted number of
975 patients in Fukuoka Prefecture in 2018. The black line is the daily maximum

976 temperature, the gray bar is the observed number of patients, the blue line is the
977 number of patients predicted by the benchmark model (Model 1) the green line is the
978 number of patients predicted by the model that fitted with data for each prefecture
979 (Model 3), and the orange line is the number of patients predicted by the model that
980 does consider short-term heat acclimatization (Model 5).

981

982 Fig. 5 Better explanatory variables (daily maximum temperature or daily maximum
983 WBGT) for prediction. MAE is used as an evaluation criterion for prediction accuracy.
984 Model 6 was used. Green: Prefectures where the daily maximum temperature model
985 produces higher prediction accuracy. Blue: Prefectures where the daily maximum
986 WBGT model produces higher prediction accuracy. White: Prefectures where the
987 difference in the prediction between the daily maximum temperature model and the
988 daily maximum WBGT model is 4% or less. The color shading represents $(1 - (\text{MAE of the model with high accuracy}) / (\text{MAE of the model with low accuracy})) * 100$ (%).

990

991 Fig. 6 Better explanatory variables (daily maximum temperature or daily maximum WBGT)
992 for prediction. RMSE is used as an evaluation criterion for prediction accuracy. Model
993 6 was used. Green: Prefectures where the daily maximum temperature model
994 produces higher prediction accuracy. Blue: Prefectures where the daily maximum
995 WBGT model produces higher prediction accuracy. White: Prefectures where the
996 difference in the prediction between the daily maximum temperature model and the
997 daily maximum WBGT model is 4% or less. The color shading represents $(1 - (\text{RMSE of the model with high accuracy}) / (\text{RMSE of the model with low accuracy})) * 100$ (%).

999

1000 Fig. 7 The number of patients with heatstroke per 10,000 people (average per summer)
1001 during the baseline period (1981-2000) estimated by the prediction model.

1002

1003 Fig. 8 Predicted number of patients with heatstroke (per 10,000 population) under the near-
1004 future climate under the RCP8.5 scenario, using daily maximum temperature as the
1005 explanatory variable. (a) prediction without population dynamics (Case 1), (b) prediction
1006 with population dynamics (Case 2), (c) prediction using the late summer equation (Case
1007 3a), and (d) prediction using the climate analog (Case 3b). The areas shaded by gray
1008 color are outside of analysis target.

1009

1010

1011 Fig.9 The rate of increase in the number of patients with heatstroke in Japan from baseline
1012 to the near future. Relative value when the number of patients with heatstroke during
1013 the Baseline period is set to 1.

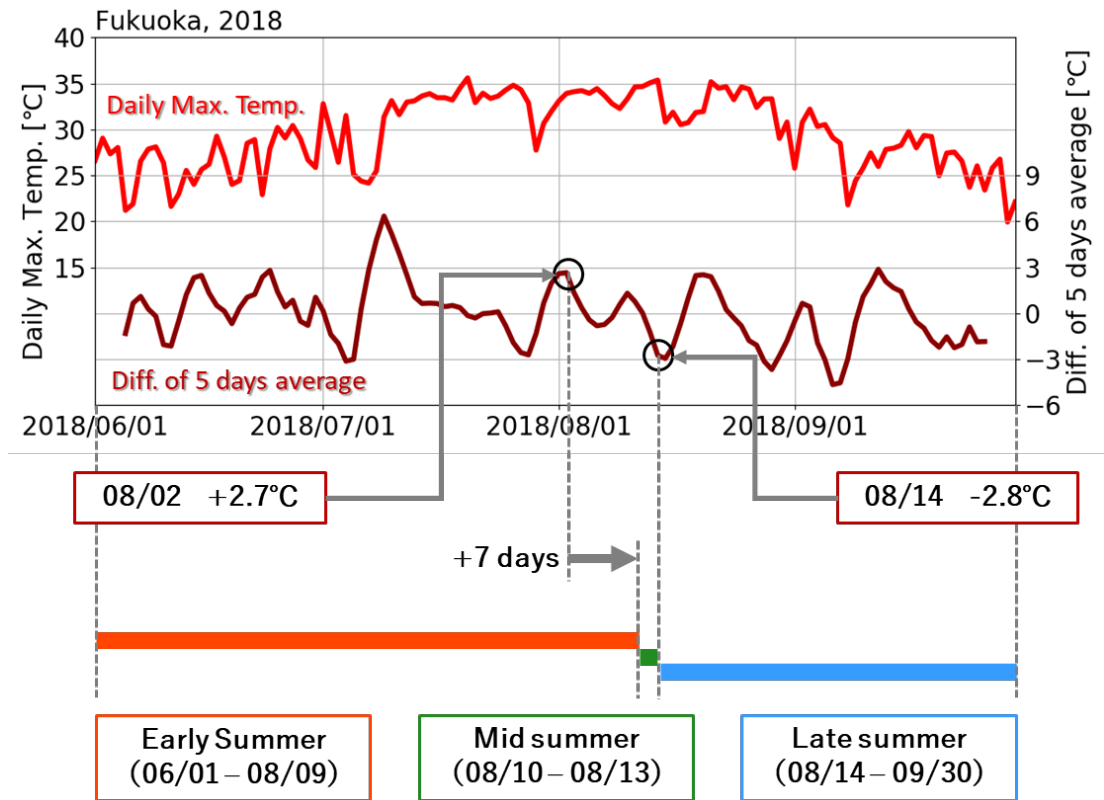
1014

1015 Fig. 10 The rate of increase in the patients with heatstroke from baseline period to the near
1016 future (RCP8.5 scenario) using daily maximum temperature as the explanatory variable.
1017 (a) prediction without population dynamics (Case 1), (b) prediction with population
1018 dynamics (Case 2), (c) prediction using the late summer equation (Case 3a), and (d)
1019 prediction using the climate analog (Case 3b). The areas shaded by gray color are
1020 outside of analysis target.

1021

1022 Fig.11 Predicted number of patients with heatstroke (per 10,000 population) under the
1023 RCP8.5 scenario near-future climate with daily maximum WBGT as explanatory variable.
1024 (a) prediction without population dynamics (Case 1), (b) prediction with population
1025 dynamics (Case 2), (c) prediction using the late summer equation (Case 3a), and (d)
1026 prediction using the climate analog (Case 3b). The areas shaded by gray color are
1027 outside of analysis target.

1028

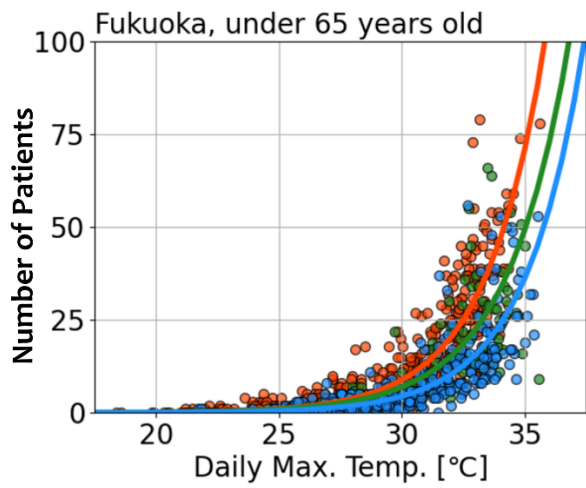


1029

1030

1031 Fig. 1 An example of period division used in this study.

1032

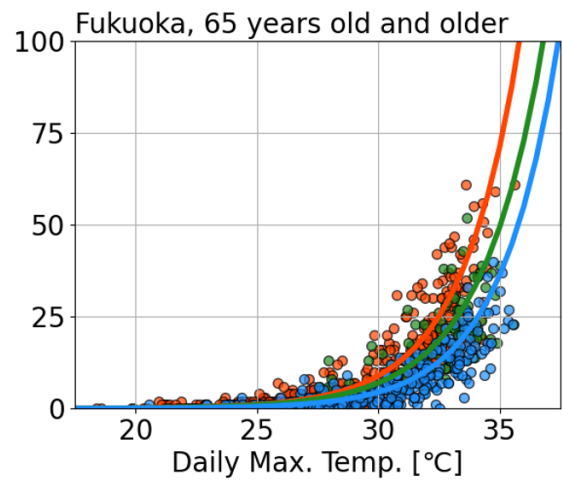


1033

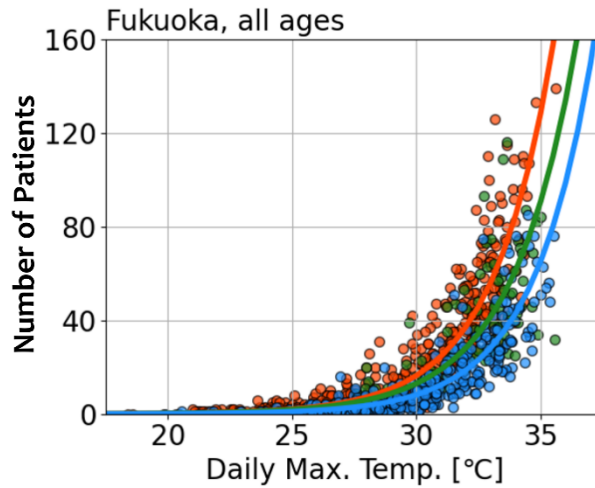
1034

1035

(a)



(b)



1036

1037

1038

(c)

1039

1040

1041

1042

1043

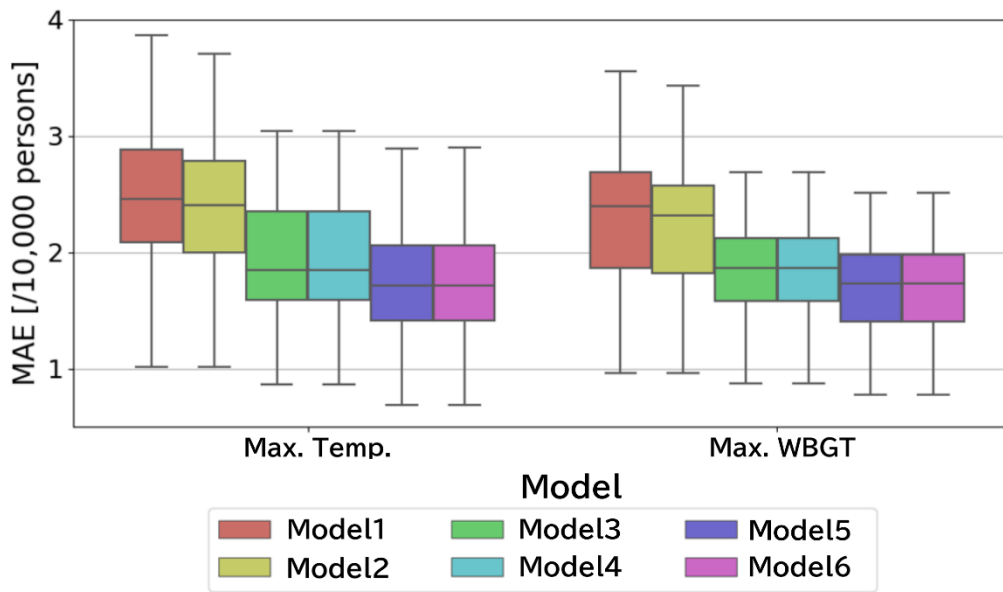
1044

1045

1046

Fig. 2 Scatterplot showing the relationship between the daily maximum temperature and the number of patients in Fukuoka Prefecture in 2018. Red, green, and blue plots indicate early summer, mid-summer, and late summer periods, respectively. The lines are prediction equations fitted from the data indicated by the plots. The scatterplot (a) shows the number of patients who are under 65 years of age. The scatterplot (b) shows the number of patients who are 65 years of age or older. The scatterplot (c) shows the number of patients who are all ages.

1047

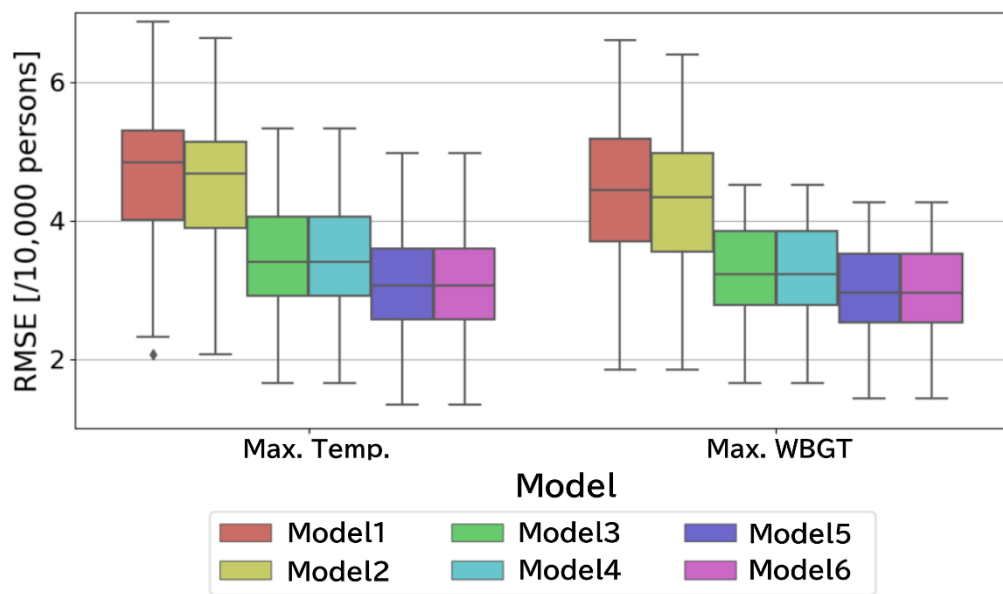


1048

1049

1050

(a)



1051

1052

1053

(b)

1054

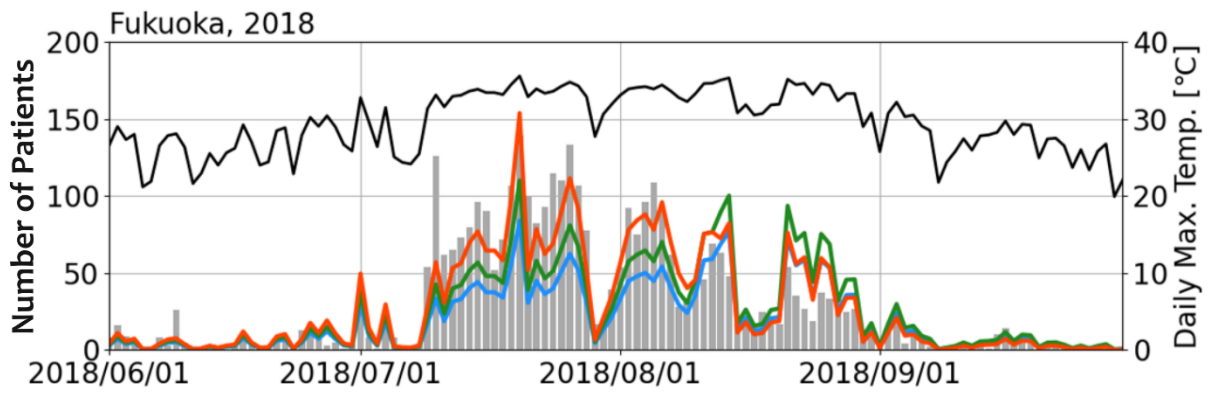
1055

1056

1057

Fig. 3 (a) MAE and (b) RMSE of the number of patients in 2018 predicted using each model. Box whiskers represent the range in values obtained for 46 regions. To remove the effect of population size, MAE and RMSE were plotted as normalized values per 10,000 people.

1058
1059



1060

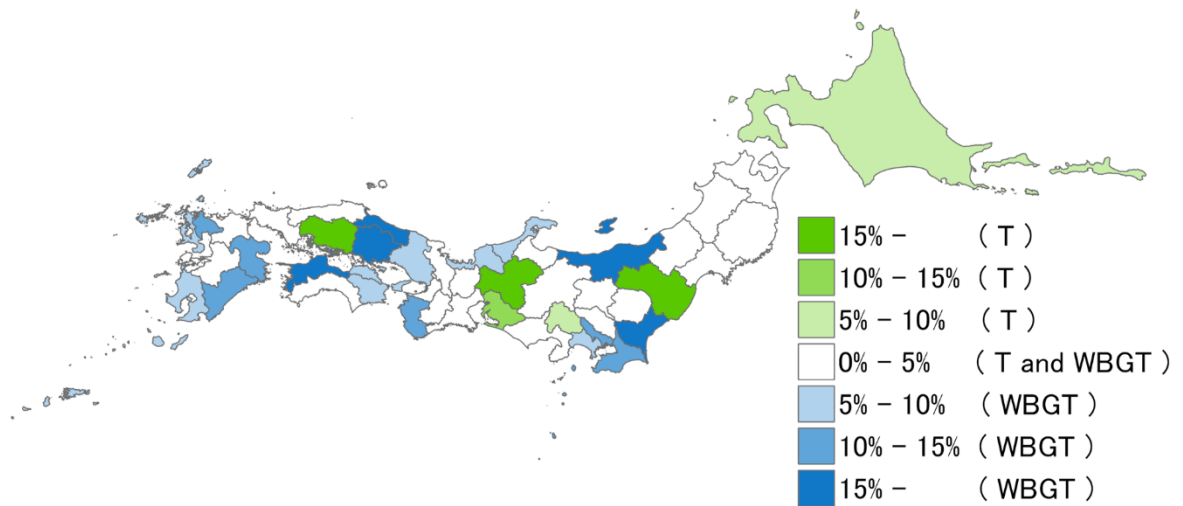
1061

1062 Fig. 4 Time series of the daily maximum temperature and actual and predicted number of
1063 patients in Fukuoka Prefecture in 2018. The black line is the daily maximum
1064 temperature, the gray bar is the observed number of patients, the blue line is the
1065 number of patients predicted by the benchmark model (Model 1), the green line is the
1066 number of patients predicted by the model that fitted with data for each prefecture
1067 (Model 3), and the orange line is the number of patients predicted by the model that
1068 does consider short-term heat acclimatization (Model 5).

1069

1070

1071



1072

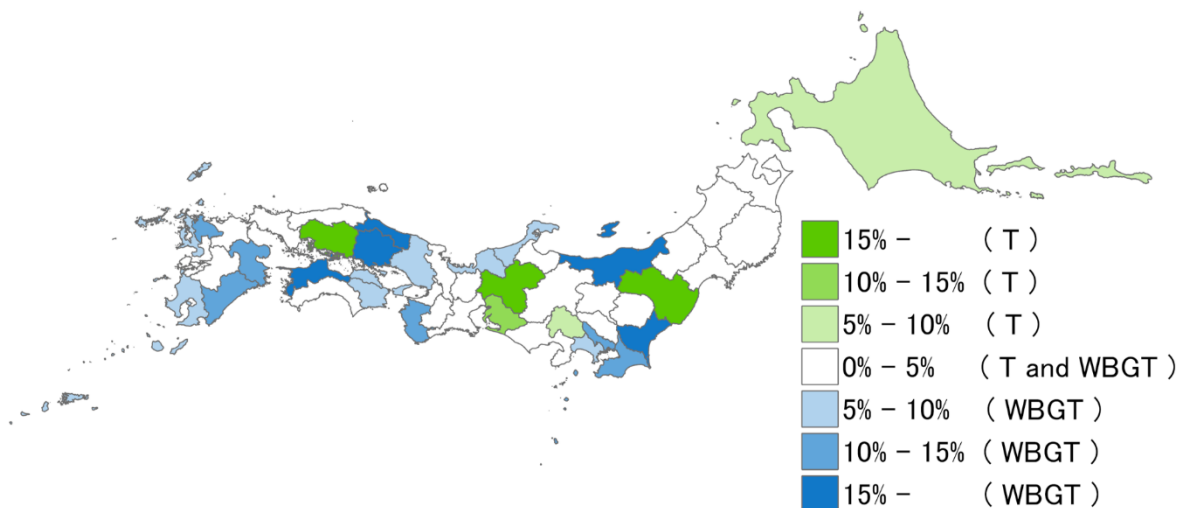
1073

1074 Fig. 5 Better explanatory variables (daily maximum temperature or daily maximum
1075 WBGT) for prediction. MAE is used as an evaluation criterion for prediction accuracy.
1076 Model 6 was used. Green: Prefectures where the daily maximum temperature model
1077 produces higher prediction accuracy. Blue: Prefectures where the daily maximum
1078 WBGT model produces higher prediction accuracy. White: Prefectures where the
1079 difference in the prediction between the daily maximum temperature model and the
1080 daily maximum WBGT model is 4% or less. The color shading represents $(1 - (\text{MAE of the model with high accuracy}) / (\text{MAE of the model with low accuracy})) * 100$ (%).

1082

1083

1084



1085

1086

1087 Fig. 6 Better explanatory variables (daily maximum temperature or daily maximum WBGT)

1088 for prediction. RMSE is used as an evaluation criterion for prediction accuracy. Model

1089 6 was used. Green: Prefectures where the daily maximum temperature model

1090 produces higher prediction accuracy. Blue: Prefectures where the daily maximum

1091 WBGT model produces higher prediction accuracy. White: Prefectures where the

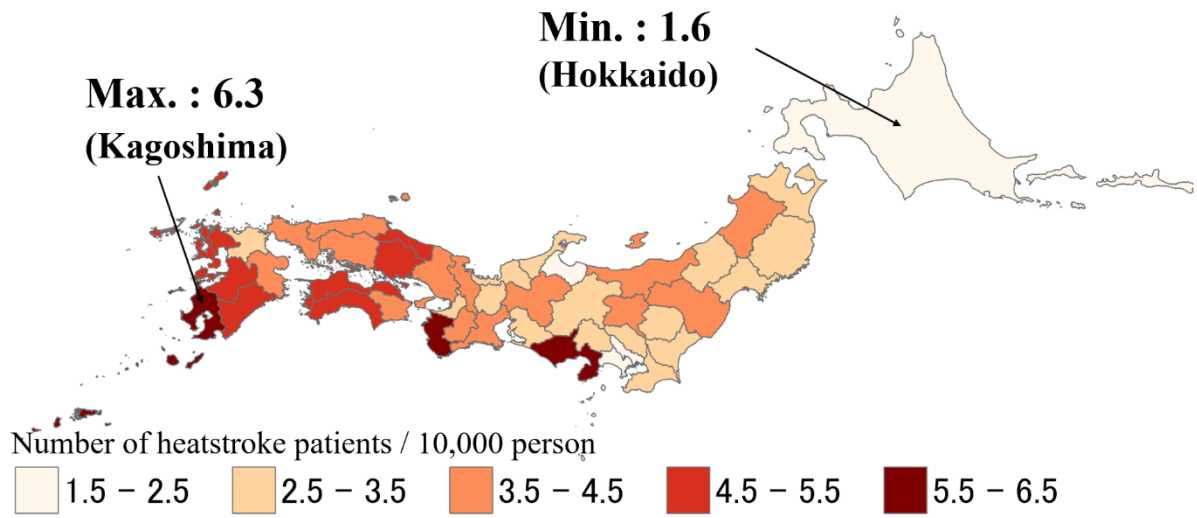
1092 difference in the prediction between the daily maximum temperature model and the

1093 daily maximum WBGT model is 4% or less. The color shading represents $(1 - (\text{RMSE of the model with high accuracy}) / (\text{RMSE of the model with low accuracy})) * 100$ (%).

1094

1095

1096



1098

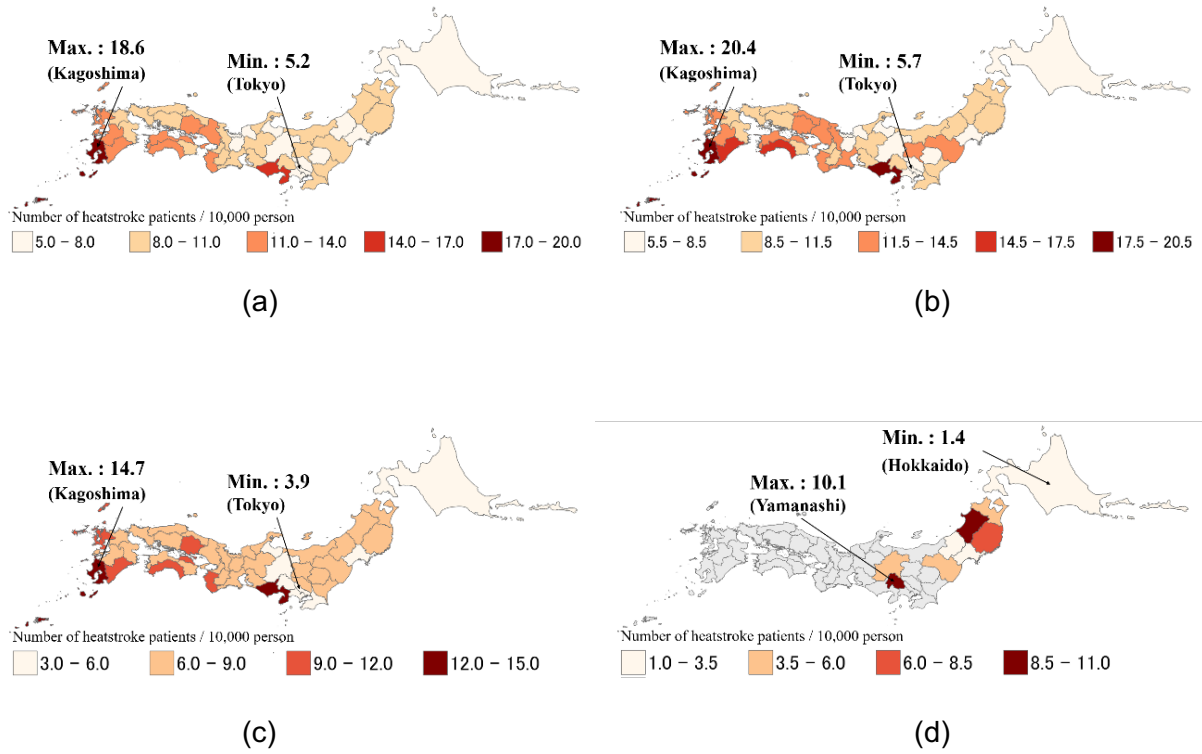
1099

1100 Fig. 7 The number of patients with heatstroke per 10,000 people (average per summer)
1101 during the baseline period (1981-2000) estimated by the prediction model.

1102

1103

1104



1105
1106
1107
1108
1109

1110

1111

1112

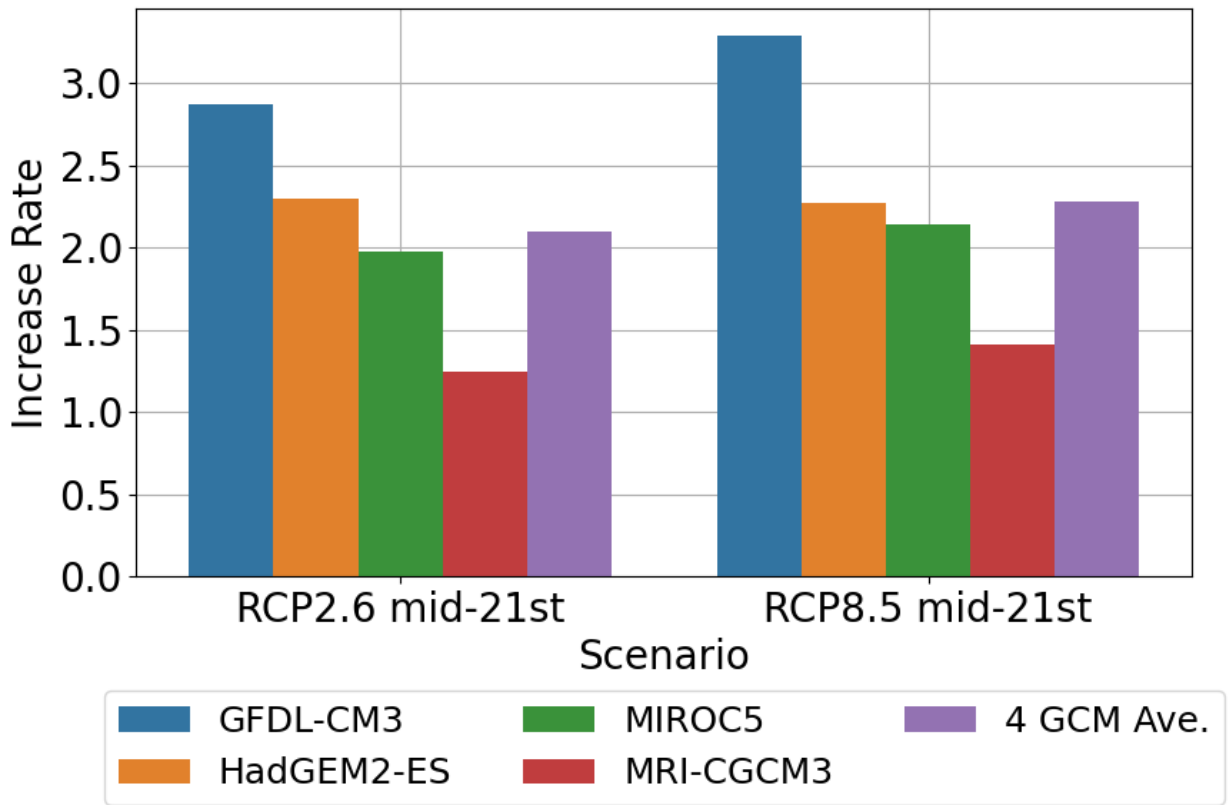
1113

1114 Fig. 8 Predicted number of patients with heatstroke (per 10,000 population) under the near-
1115 future climate under the RCP8.5 scenario, using daily maximum temperature as the
1116 explanatory variable. (a) prediction without population dynamics (Case 1), (b) prediction
1117 with population dynamics (Case 2), (c) prediction using the late summer equation (Case
1118 3a), and (d) prediction using the climate analog (Case 3b). The areas shaded by gray
1119 color are outside of analysis target.

1120

1121

1122



1124

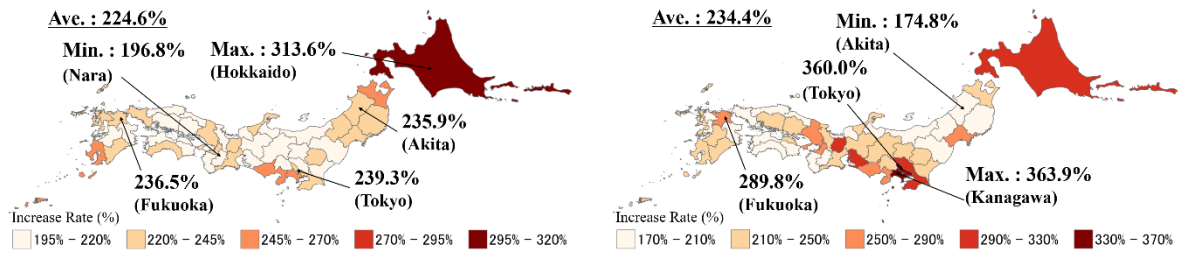
1125

1126 Fig.9 The rate of increase in the number of patients with heatstroke in Japan from baseline
 1127 to the near future. Relative value when the number of patients with heatstroke during
 1128 the Baseline period is set to 1.

1129

1130

1131



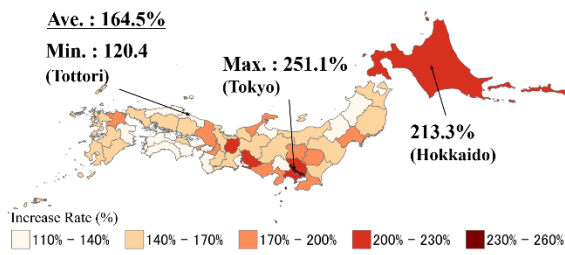
1132

1133

1134

(a)

(b)

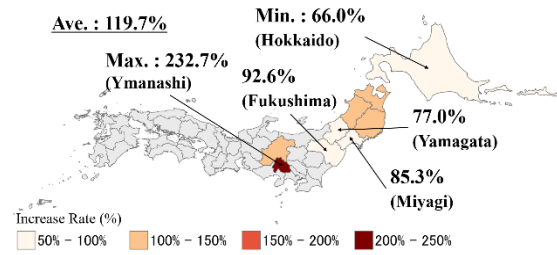


1135

1136

1137

(c)



(d)

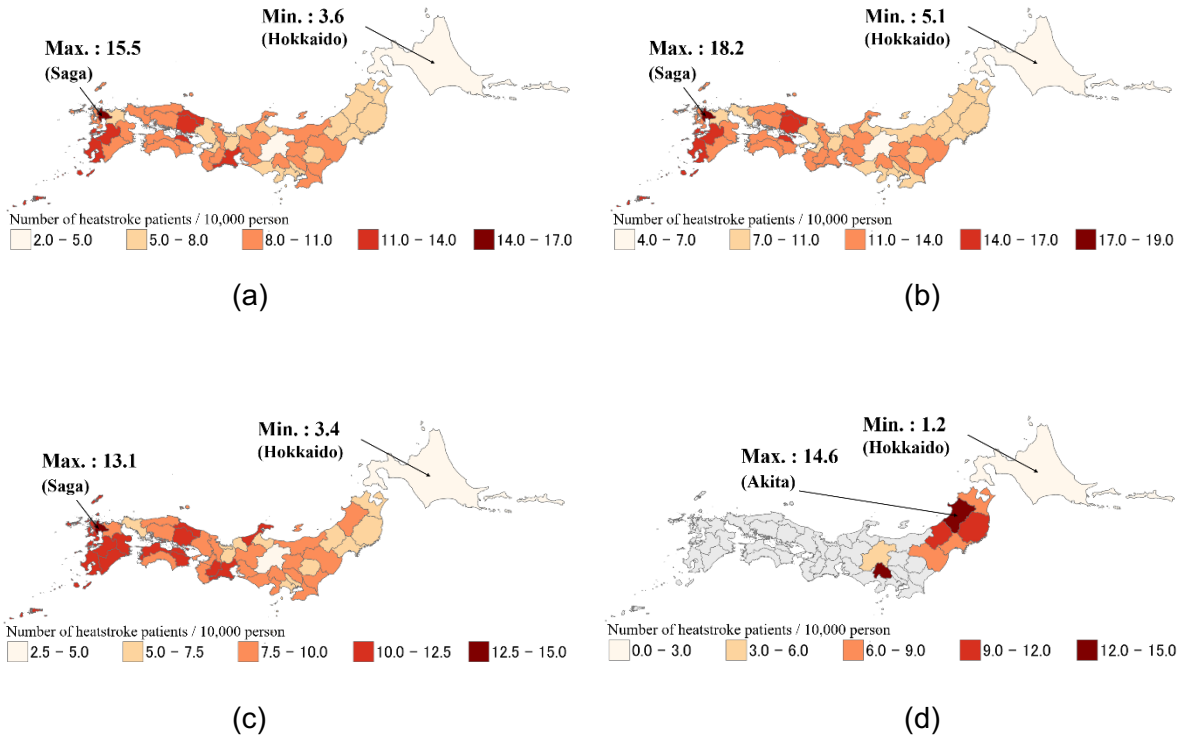
1138 Fig. 10 The rate of increase in the patients with heatstroke from baseline period to the near
 1139 future (RCP8.5 scenario) using daily maximum temperature as the explanatory variable.
 1140 (a) prediction without population dynamics (Case 1), (b) prediction with population
 1141 dynamics (Case 2), (c) prediction using the late summer equation (Case 3a), and (d)
 1142 prediction using the climate analog (Case 3b). The areas shaded by gray color are
 1143 outside of analysis target.

1144

1145

1146

1147



1148
1149
1150
1151
1152

1153

1154
1155

1156 Fig.11 Predicted number of patients with heatstroke (per 10,000 population) under the
1157 RCP8.5 scenario near-future climate with daily maximum WBGT as explanatory variable.
1158 (a) prediction without population dynamics (Case 1), (b) prediction with population
1159 dynamics (Case 2), (c) prediction using the late summer equation (Case 3a), and (d)
1160 prediction using the climate analog (Case 3b). The areas shaded by gray color are
1161 outside of analysis target.

1162

1163

1164

List of Tables

1165

1166

1167

1168 Table 1 List of models that were compared for accuracy.

1169

1170 Table 2 List of future projection experiments and featured factor.

1171

1172 Table 3 Patterns of change in population and increase/decrease in risk of heat stroke
1173 emergencies from baseline period to near future.

1174

1175

1176

1177 Table 1 List of models that were compared for accuracy.

1178

1179

	Fitted Data			Period Division	Age Group
	Tokyo	Each Prefecture			
Model 1	○				
Model 2	○				○
Model 3		○			
Model 4		○			○
Model 5		○		○	
Model 6		○		○	○

1180

1181

1182

1183

1184

1185 Table 2 List of future projection experiments and featured factor.

1186

1187

1188

	Climate Change Scenarios	Population	Long-term Acclimatization
Case 1	RCP 8.5	1990	—
Case 2	RCP 8.5	2040	—
Case 3a	RCP 8.5	2040	Late summer equation
Case 3b	RCP 8.5	2040	Climate analog

1189

1190

1191

1192

1193

1194

1195 Table 3 Patterns of change in population and increase/decrease in risk of heatstroke

1196 emergencies from baseline period to near future.

1197

1198

The proportion of elderly people in the total population			
	Increase	Decrease	
Population	Increase	Prefectures at increased risk : 6	—
		Prefectures at increased risk : 20	
	Decrease		—
		Prefectures at decreased risk : 20	

1199

1200

1201

1202